

**STUDY OF HEAT TRANSFER  
CHARACTERISTICS OF COMPACT  
HEAT EXCHANGER DURING START  
UP**

A Thesis

Submitted to the College of Engineering  
of Nahrain University in Partial Fulfillment  
of the Requirements for the Degree of  
Master of Science  
in  
Chemical Engineering


by

**NIBRAS HASANI OLEWI AL-OBAIDI**  
**(B.Sc. in Chemical Engineering 2004)**

January	2008
Moharam	1429

## Certification

I certify that this thesis entitled "**Study of Heat Transfer Characteristics of Compact Heat Exchanger During Start Up**" was prepared by "**Nibras Hasani Olewi Al-Obaidi**" under my supervision at Nahrain University/ College of Engineering in partial fulfillment of the requirements for the degree of Master of Science in Chemical engineering.

Signature: 

Name: Dr. Naseer A. Al-Habbobi

(Supervisor)

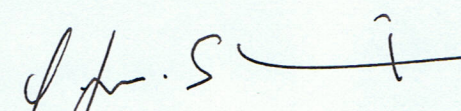
Date: 16 / 3 / 2008

Signature:  
Name: Asst. Prof. Dr. Qasim J. M. Slaiman

(Supervisor)

Date: 16 / 3 / 2008

Approval of the College of Engineering

Signature: 

Name: Prof. Dr. Qasim J. M. Slaiman

(Head of department)

Date: 16 / 3 / 2008


Signature:  
Name: Prof. Dr. Muhsin J. Jweeg


(Acting Dean)


Date: 3 / 14 / 2008

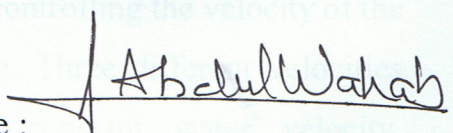
### Certificate

We certify, as an examining committee, that we have read this thesis entitled **“Study of Heat Transfer Characteristics of Compact Heat Exchanger During Start Up”** , examined the student **“Nibras Hasani Olewi Al-Obaidi ”** in its content and found it meets the standard of thesis for the degree of Master of Science in Chemical Engineering.

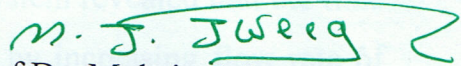
Signature :   
Name : Dr. Naseer A. Al-Habbobi  
(Supervisor)  
Date : 16 / 3 / 2008

Signature:   
Name : Dr. Basim O. Hasan  
(Member)  
Date : 16 / 3 / 2008

Signature :   
Name : Assist. Prof. Dr. Cecilia K.  
Haweel  
(Supervisor)  
Date : 16 / 3 / 2008

Signature :   
Name : Assist. Prof. Dr. Majid I.  
Abdul-Wahab  
(Chairman)  
Date : 16 / 3 / 2008

Approval of the College of Engineering

Signature:   
Name : Prof. Dr. Muhsin J. Jweeg  
(Acting Dean)  
Date : 3 / 14 / 2008

## **Abstract**

Compact heat exchangers have been widely used in various applications in thermal fluid systems including automotive thermal management systems. Radiators for engine cooling systems, evaporators and condensers for HVAC systems, oil coolers, and intercooler which are typical examples of the compact heat exchangers that can be found in ground vehicles. Compact heat exchangers are used in low heat transfer rates of gas-liquid systems because of the high surface area per unit volume of this device. It is used to transfer heat in system characterized by low heat transfer coefficient.

In this work, a compact heat exchanger of 20x19x5cm has been used with hot water of 60°C flowing inside the heat exchanger and air at room temperature flowing across it. A fan is located with a small tunnel adjacent to the heat exchanger. The velocity of fan can be controlled by a Voltage switch. Changing velocity of air by controlling the velocity of the fan which increase flow rate of air flowing. Three different velocities have been studied in this work with constant water velocity. Thermometers are used to register temperature variation with time for outlet streams.

It is found that the main factor which affects the heat transfer is the heat transfer coefficient of air side which can be increased by increasing the flow rate of air while water flow rate has minor effect on the heat transfer operation. The effectiveness also behaves in the same way and it could be increased as well by increasing the air flow rate.

Studying the dynamic response of the system revealed that the time constant for such system could be decreased by increasing flow rate of

air, which means faster dynamic temperature response. The dead time drops steeply as the flow rate of air increases.

## List of Contents

<u>Contents</u>	<u>Pages</u>
Abstract	I
List of Contents	III
Notations	V
List of Tables	VII
List of Figures	VIII
 <b><u>Chapter One: General Introduction</u></b>	
1.1 Introduction	1
1.2 Scope of Thesis	3
 <b><u>Chapter Two: Literature Survey of Compact Heat Exchanger</u></b>	
2.1 Introduction	4
2.2 Criteria for Selection	4
2.3 Types of Compact Heat Exchangers	6
2.4 Design for Some Types of Compact Heat Exchanger	20
2.5 Heat Transfer Aspects of Compactness	26
2.6 Effectiveness – NTU Method	30
2.7 Functional Form of the Overall Heat Transfer Coefficient	31
2.8 Previous Work	33
 <b><u>Chapter Three: Experimental Work</u></b>	
3.1 Introduction	38
3.2 Components of Test System	38
3.3 Test Measuring Parameters and Procedure	31
3.4 Test Results	41
3.5 Control of the Heat Exchanger	43
 <b><u>Chapter Four: Calculation and Interpretation</u></b>	
4.1 Theoretical Calculations of the Heat Exchanger Parameters	45

4.2 Control of Heat Exchanger	53
<b><u>Chapter Five: Discussions</u></b>	
5.1 Discussion of NTU Method	64
5.2 Discussion of the Control of Heat Exchanger	66
<b><u>Chapter Six: Conclusions and Recommendations</u></b>	
6.1 Conclusions	68
6.2 Recommendations	68
References	70
Appendices	

## NOTATIONS

<b>Symbol</b>	<b>Definition</b>	<b>Unit</b>
A	Area	m <sup>2</sup>
A <sub>c</sub>	Flow area	m <sup>2</sup>
C <sub>p</sub>	Specific heat capacity	J/Kg.°C
h	Heat transfer coefficient	W/m <sup>2</sup> .°C
ID	Inside diameter	m
J	Colburn Factor	-
k	Conductivity	W/m.°C
m'	Mass flow rate	Kg/s
n	No. of pipes	-
Nu	Nusselt no.	-
OD	Outside diameter	m
Q	Volumetric flow rate	m <sup>3</sup> /s
q	Heat Transfer Rate	Watt
Pr	Prandtl no.	-
Re	Reynolds no.	-
S <sub>t</sub> ,S <sub>1</sub> ,s	Shape factor	-
St	Stanton no.	-
T	Temperature	°C
T <sub>i</sub> <sup>R</sup> (t)	Unsteady state dynamic response	-
U	Overall heat transfer coefficient	W/m <sup>2</sup> .°C
u	Velocity	m/s
V <sub>s</sub>	Enclosed (wetted) volume	m <sup>3</sup>
W	Width of the Plate	m



## Greek Symbols

$\varepsilon$	Effectiveness	-
$\theta$	Dead or delay time	sec
$\tau$	Time constant	sec
$\Lambda$	Darcy Factor	-

## List of Tables

<b>Table</b>	<b>Title</b>	<b>Page</b>
3.1	Specifications of First Test	41
3.2	Results of the First Test	42
3.3	Specifications of Second Test	42
3.4	Results of the Second Test	42
3.5	Specifications of Third Test	43
3.6	Results of the Third Test	43
4.1	Theoretical Values of U	47
4.2	Air Side Heat Transfer Coefficient	49
4.3	Air Temperature Response with Time For 1 <sup>st</sup> Test	53
4.4	Water Temperature Response with Time For 1 <sup>st</sup> Test	55
4.5	Air Temperature Resp. with Time For 2nd Test	57
4.6	Water Temperature Resp. with Time For 2nd Test	58
4.7	Air Temperature Response with Time For 3d Test	60
4.8	Water Temperature Resp. with Time For 3d Test	62
5.1	Time Constant & Dead Time for Air Side T.R.	67
A1	Properties of Air at Atmospheric Pressure	A1
A2	Properties of Water	A2

## List of Figures

<b>Figure</b>	<b>Title</b>	<b>PAGE</b>
2.1	Exploded view of a gasketed-plate heat exchanger	9
2.2	Brazed stainless steel exchanger	11
2.3	A compact spiral heat exchanger	13
2.4	Basic structure of plate heat exchanger	16
2.5	Overview of compact heat transfer surfaces	30
3.1	Schematic diagram of the system	39
3.2a	View of the system	40
3.2b	View of the system	41
4.1	Air Heat transfer coefficient vs. air volumetric flow rate	50
4.2	Overall heat transfer coefficient change with volumetric flow rate of air.	51
4.3	Overall heat transfer coefficient change with volumetric flow rate of water	51
4.4	Effectiveness versus air flow rate at different water flow rates.	52
4.5	Air temperature response for the first test	54
4.6	Experimental and dynamic T.R. of air for the first test.	54
4.7	Water temperature response for the first test.	55
4.8	Experimental and dynamic Temperature response of water for the first test	56
4.9	Air temperature response for the second test.	57
4.10	Experimental and dynamic temperature response of air for the second test.	58
4.11	Water temperature response for the second test	59
4.12	Experimental and dynamic temperature response of water for the second test	60
4.13	Air temperature response for the third test	61

4.14	Experimental and dynamic temperature response of air for the third test	61
4.15	Water temperature response for the third test	62
4.16	Experimental and dynamic temperature response of water for the third test	63

# Chapter One

## Introduction

### 1.1 Introduction

Compact heat exchangers have been widely used in various applications in thermal fluid systems including automotive thermal management systems. Radiators for engine cooling systems, evaporators and condensers for HVAC systems, oil coolers, and intercooler are typical examples of the compact heat exchangers that can be found in ground vehicles [1]. Compact heat exchangers are used in low heat transfer rates of gas-liquid systems because of the high surface area per unit volume of this device [2]. A heat exchanger is a complex device that provides the transfer of thermal energy between two or more fluids at different temperatures. Heat exchangers are used, either individually or as components of larger thermal systems, in a wide variety of industrial, commercial and household applications, e.g. refrigeration, ventilating and air-conditioning systems, power generation, process, manufacturing and space industries, as well as in environmental engineering. Although a wide variety of heat exchangers exists in the market, the present thesis will concentrate in the commonly used compact heat exchanger. The complexity of these systems stems from their geometrical configuration, the physical phenomena present in the transfer of heat, and the large number of variables involved in their operation, presently, the vast majority of the analyses for predicting their behavior include assumptions and conditions that are not consistent with the phenomena occurring in them under actual states of operation. The shortcomings in the current approach thus lead, in many cases, to unsatisfactory predictions of the heat transfer with errors that can be sometimes of the order of 25–30% or

higher. Since heat exchanger performance is very often a key factor in the overall thermal system design, constant improvements in their modeling and simulation are definitely needed to increase the accuracy of their predictions and, consequently, to improve the reliability and efficiency of thermal systems for the specific application [3]. Heat exchangers play an essential role in chemical processing. In the typical process plant, heat exchangers bring the feed streams to the proper temperature for the reactors, provide vapor and liquid reflux streams for the separation and purification steps, and finally cool the products for storage and shipping. But the same types of heat exchangers are used in a wide variety of auxiliary services in process plants and many other places as well; examples include lubricating-oil coolers for all kinds of machinery, compressor intercoolers and after coolers for gas pipeline systems, chillers in refrigeration and air-conditioning installations, and vapor generators and condensers in conventional, nuclear, geothermal, and solar thermal power plants [4].

Heat exchangers come in many different configurations and with surface areas ranging from 0.1 to 100,000 m<sup>2</sup>. The selection of type or configuration of heat exchanger is governed by the nature of the streams flowing in the exchanger (e.g., liquid or gas, high or low pressure, high or low temperature) and the service (e.g., heating or cooling, condensing, vaporizing) to be performed [5]. The size of the heat exchanger is governed by the amount of heat to be transferred and the rate of heat transfer, which can vary by several orders of magnitude [2]. The use of soft computing technologies has received much attention in recent years as an alternative approach to cope with real-world problems. It has been used in a wide variety of applications in both the natural and engineering sciences, among which are decision making, pattern recognition, system control, information processing, natural languages, optimization, speech

recognition, vision and robotics. The excellent inherent characteristics provided by these methodologies allow them to recognize and model the nonlinear phenomena present in complex processes. A main advantage provided by soft computing stems from the fact that its constituent methodologies are for the most part complementary and synergistic rather than competitive, and can be combined to increase even more the quality of their results [6]. The design of finned-tube heat exchangers requires specification of more than a dozen parameters, including but not limited to the following: transverse tube spacing, longitudinal tube spacing, tube diameter, number of tube rows, fin spacing, fin thickness, and fin type (plain or enhanced). Circuiting is another important specification that will affect performance of a finned-tube heat exchanger [7]

## **1.2 Scope of the Thesis**

In this work it is attempted to study the factors which have the biggest effect on heat transfer rates in a compact heat exchanger. The effect of flow rates variation of water and air has been studied on overall heat transfer coefficient and effectiveness of the application. Dynamic study of control variables and responses has been reviewed and the effect of flow rate on them. The optimum conditions for operating of compact heat exchanger have been studied. Chapter one is a general introduction of compact heat exchangers. Chapter two is a literature review for the types and design equations of all types of compact heat exchangers. Chapter three is a description of the apparatus, working conditions and experimental results. Chapter four is the simulation of results and a study of dynamic response of the system. Chapter five is the discussion of the results and chapter six is the conclusions and recommendations for future work.

## **Chapter Two**

### **Literature Survey of Compact Heat Exchanger**

#### **2.1 Introduction**

With equipment costs rising and limited available plot space, compact heat exchangers are gaining a larger portion of the heat exchange market. Numerous types use special enhancement techniques to achieve the required heat transfer in smaller plot areas and, in many cases, less initial investment. As with all items that afford a benefit there is a series of restrictions that limit the effectiveness or application of these special heat exchanger products. In most products discussed some of these considerations are presented, but a thorough review with reputable suppliers of these products is the only positive way to select a compact heat exchanger [8].

#### **2.2 Criteria for Selection**

Given the large variety of process heat transfer problems and the heat exchanger configurations available, the engineer must select a type and design that satisfy several criteria. These are listed approximately in the order of their importance, though in any individual case one criterion or another may move up or down in the list of relative importance. [9]

1. The heat exchanger must satisfy process specifications; that is, it must perform the required thermal change on the process stream within the pressure drop limitations imposed. The basic thermal design equations are discussed in a later section, and these determine the size of the heat exchanger. Equally important to a successful design is the proper utilization of the allowed pressure drops for each stream. As a general rule, the greater the allowable pressure drop, the higher the fluid velocity and heat transfer



coefficient, resulting in a smaller and less expensive heat exchanger. However, pressure drop increases with fluid velocity more rapidly than does heat transfer, and pumping costs soon become prohibitive. Also, excessive velocities can cause damage by cavitations, erosion, and vibration. Therefore, the allowable pressure drop in each stream should be carefully chosen (70 kPa is a typical value for low-viscosity liquids, and 5–10% of the absolute pressure is typical for low-pressure gases and vapors), and as fully utilized as other considerations permit.

2. The heat exchanger must withstand service conditions. The most obvious condition is that the exchanger construction must be strong enough to contain the fluid pressures inside the exchanger, and design standards for safe construction are set by the various pressure-vessel codes. There are also thermally induced stresses due to the differential expansion of the various exchanger components. There are mechanical stresses imposed by the exchanger weight and externally by piping stresses, wind loading, and mechanical handling during shipping, installation, and maintenance. The heat exchanger must withstand corrosive attack, primarily achieved by suitable selection of the materials of construction. To minimize erosion and vibration problems, it is important to limit velocities, especially in certain critical areas near the nozzles and wherever the flow is forced to change direction in the heat exchanger. The exchanger must also be designed either to minimize fouling or to withstand the mechanical effects as fouling does develop.

3. The heat exchanger must be maintainable. It must allow mechanical or chemical cleaning if the heat transfer surface becomes fouled, and it must permit replacement of the tubes, gaskets, and any other components that may fail or deteriorate during the normal lifetime of the exchanger. Maintenance should be accomplished with minimum downtime and handling difficulties and labor cost.

4. Operational flexibility. The heat exchanger and its associated piping and control system must permit operation over the probable range of conditions without instability, excessive fouling, vibration problems, or freeze-up that might damage the exchanger itself. Both changes in process conditions (e.g., changes in process flow rate or composition) and in environmental conditions (e.g., daily and seasonal changes in atmospheric temperature) must be considered.
5. Cost. Cost considerations must include not only delivered cost and installation, but particularly the cost of lost production. The value of products from a process plant is generally so much greater than the cost of any one piece of equipment that loss of production due to inadequate equipment capacity or excessive downtime quickly out-weighs any capital cost savings achieved by undersizing equipment.
6. Other design criteria include maximum weight, length, and/or diameter limitations to facilitate installation and maintenance. Use of standard replaceable components minimizes inventory [6].

## **2.3 Types of Compact Heat Exchangers**

### **2.3.1 PLATE-AND-FRAME EXCHANGERS**

There are two major types gasketed and welded-plate heat exchangers.

Each shall be discussed individually.

#### **2.3.1.1 GASKETED-PLATE EXCHANGERS (G. PHE)**

This type is the fastest growing of the compact exchangers and the most recognized as shown in Fig. 2.1. A series of corrugated alloy material channel plates, bounded by elastomeric gaskets are hung off and guided by longitudinal carrying bars, then compressed by large-diameter tightening bolts between two pressure retaining frame plates (cover plates). The frame and

channel plates have portholes which allow the process fluids to enter alternating flow passages (the space between two adjacent-channel plates). Gaskets around the periphery of the channel plate prevent leakage to the atmosphere and also prevent process fluids from coming in contact with the frame plates. No interfluid leakage is possible in the port area due to a dual-gasket seal. The frame plates are typically epoxy-painted carbon-steel material and can be designed per most pressure vessel codes. The channel plates are always an alloy material with 304SS as a minimum. Channel plates are typically 0.4 to 0.8 mm thick and have corrugation depths of 2 to 10 mm. Special Wide Gap (WG PHE) plates are available, in limited sizes, for slurry applications with depths of approximately 16 mm. The channel plates are compressed to achieve metal-to-metal contact for pressure-retaining integrity. These narrow gaps and high number of contact points which change fluid flow direction, combine to create a very high turbulence between the plates. This means high individual-heat-transfer coefficients (up to  $14200\text{W/m}^2\text{ }^\circ\text{C}$ ), but also very high pressure drops per length as well. To compensate, the channel plate lengths are usually short, most under 2 and few over 3 meters in length. In general, the same pressure drops as conventional exchangers are used without loss of the enhanced heat transfer. Expansion of the initial unit is easily performed in the field without special considerations. The original frame length typically has an additional capacity of 15–20 percent more channel plates (i.e., surface area). In fact, if a known future capacity is available during fabrication stages, a longer carrying bar could be installed, and later, increasing the surface area would be easily handled. When the expansion is needed, simply untighten the carrying bolts, pull back the frame plate, add the additional channel plates, and tighten the frame plate.

Most PHE applications are liquid-liquid services but there are numerous steam heater and evaporator uses from their heritage in the food industry. Industrial users typically have chevron style channel plates while some food applications are washboard style. Fine particulate slurries in concentrations up to 70 percent by weight are possible with standard channel spacing. Wide-gap units are used with larger particle sizes. Typical particle size should not exceed 75 percent of the single plate (not total channel) gap. Close temperature approaches and tight temperature control possible with PHE's and the ability to sanitize the entire heat transfer surface easily were a major benefit in the food industry.

Multiple services in a single frame are possible. Gasket selection is one of the most critical and limiting factors in PHE usage. Even trace fluid components need to be considered. The higher the operating temperature and pressure, the shorter the anticipated gasket life . Always consult the supplier on gasket selection and obtain an estimated or guaranteed lifetime. The major applications are, but not limited to, as follows:

- i) Temperature-cross applications (lean/rich solvent)
- ii) Close approaches (fresh water/seawater)
- iii) Viscous fluids (emulsions)
- iv) Sterilized surface required (food, pharmaceutical)
- v) Polished surface required (latex, pharmaceutical)
- vi) Future expansion required
- vii) Space restrictions
- viii) Barrier coolant services (closed-loop coolers)
- ix) Slurry applications (TiO<sub>2</sub>, Kaolin, precipitated calcium carbonate, and beet sugar raw juice) [8]

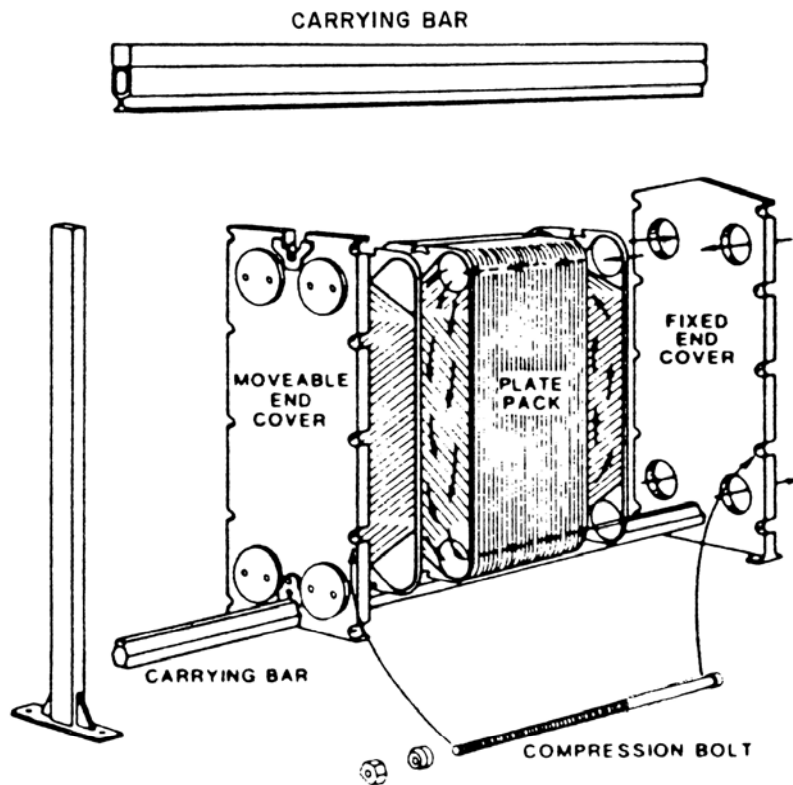


**Fig. 2.1** Exploded view of a gasketed-plate heat exchanger [8]

### **2.3.1.2 WELDED- AND BRAZED-PLATE EXCHANGERS (W. PHE & BHE)**

The title of this group of plate exchangers has been used for a great variety of designs for various applications from normal gasketed-plate exchanger services to air pre-heater services on fired heaters or boilers. The intent here is to discuss more traditional heat-exchanger designs, not the heat-recovery designs on fired equipment flue-gas streams. Many similarities exist between these products but the manufacturing techniques are quite different due to the normal operating conditions these units experience. To overcome the gasket limitations, PHE manufacturers have developed welded-plate exchangers. There are numerous approaches to this solution: weld plate pairs together with the other fluid-side conventionally gasketed, weld up both sides but use a horizontal stacking of plates method of assembly, entirely braze the

plates together with copper or nickel brazing, diffusion bond then pressure form plates and bond etched, passage plates.

Most methods of welded-plate manufacturing do not allow for inspection of the heat-transfer surface, mechanical cleaning of that surface, and have limited ability to repair or plug off damage channels. Consider these limitations when the fluid is heavily fouling, has solids, or in general the repair or plugging ability for severe services. One of the previous types has an additional consideration of the brazing material to consider for fluid compatibility. The brazing compound entirely coats both fluid's heat-transfer surfaces. The second type, a Compabloc (CP) from Vicarb, has the advantage of removable cover plates, similar to air-cooled exchanger headers, to observe both fluids surface area. The fluids flow at 90° angles to each other on a horizontal plane. LMTD correction factors approach 1.0 for Compabloc just like the other welded and gasketed PHEs. Hydroblasting of Compabloc surfaces is also possible. The Compabloc has higher operating conditions than PHE's or W-PHE.

The performances and estimating methods of welded PHEs match those of gasketed PHEs in most cases, but normally the Compabloc, with larger depth of corrugations, can be lower in overall coefficient. Some extensions of the design operating conditions are possible with welded PHEs, most notably is that cryogenic applications are possible. Pressure vessel code acceptance is available on most units.

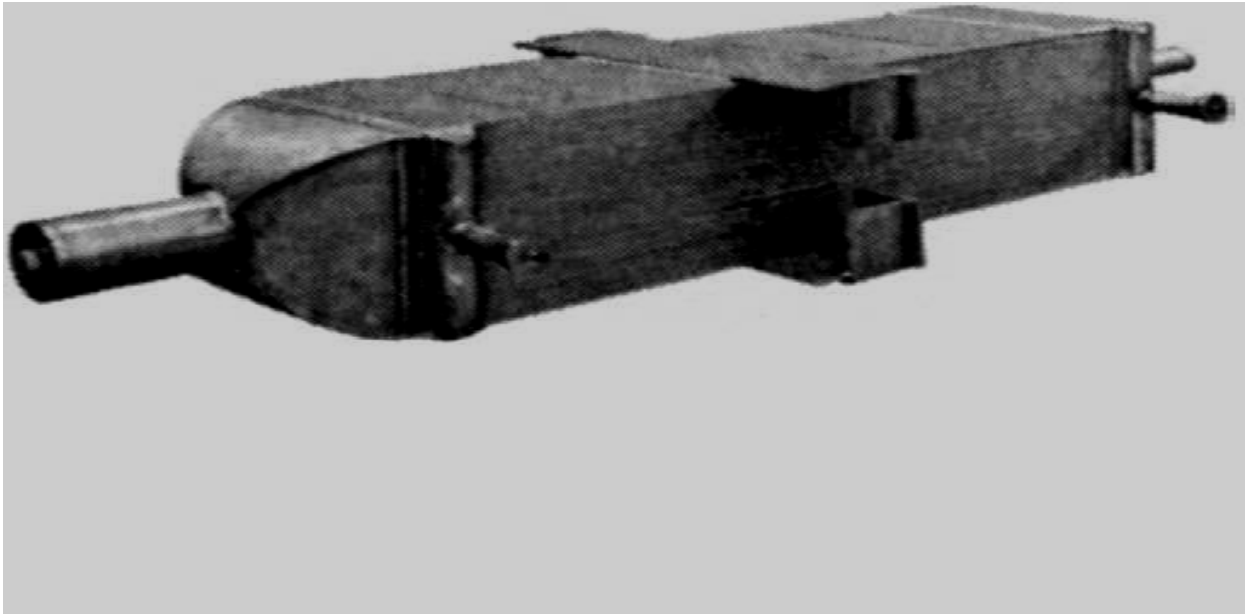


**Fig. 2.2** Brazed stainless steel exchanger [10].

### **2.3.2 SPIRAL-PLATE EXCHANGERS (SHE)**

The spiral-plate heat exchanger (SHE) may be one exchanger selected primarily on its virtues and not on its initial cost. SHEs offer high reliability and on-line performance in many severely fouling services such as slurries. The SHE is formed by rolling two strips of plate, with welded-on spacer studs, upon each other into clock-spring shape. This forms two passages. Passages are sealed off on one end of the SHE by welding a bar to the plates; hot and cold fluid passages are sealed off on opposite ends of the SHE. A single rectangular flow passage is now formed for each fluid, producing very high shear rates compared to tubular designs. Removable covers are provided on each end to access and clean the entire heat transfer surface. Pure countercurrent flow is achieved and LMTD correction factor is essentially = 1.0. Since there are no dead spaces in a SHE, the helical flow pattern combines to entrain any solids and create high turbulence creating a self-cleaning flow passage. There are no thermal-expansion problems in spirals.

Since the center of the unit is not fixed, it can torque to relieve stress. The SHE can be expensive when only one fluid requires a high alloy material. Since the heat-transfer plate contacts both fluids, it is required to be fabricated out of the higher alloy. SHEs can be fabricated out of any material that can be cold-worked and welded.

The channel spacings can be different on each side to match the flow rates and pressure drops of the process design. The spacer studs are also adjusted in their pitch to match the fluid characteristics. As the coiled plate spirals outward, the plate thickness increases from a minimum of 2 mm to a maximum (as required by pressure) up to 10 mm. This means relatively thick material separates the two fluids compared to tubing of conventional exchangers. Pressure vessel code conformance is a common request. The most common applications that fit SHE are slurries. The rectangular channel provides high shear and turbulence to sweep the surface clear of blockage and causes no distribution problems associated with other exchanger types. A localized restriction causes an increase in local velocity which aids in keeping the unit free flowing. Only fibers that are long and stringy cause SHE to have a blockage it cannot clear itself. As an additional antifoulant measure, SHEs have been coated with a phenolic lining. This provides some degree of corrosion protection as well, but this is not guaranteed due to pinholes in the lining process. There are three types of SHE to fit different applications:

**Type I** : is the spiral-spiral flow pattern. It is used for all heating and cooling services and can accommodate temperature crosses such as lean/rich services in one unit. The removable covers on each end allow access to one side at a time to perform maintenance on that fluid side. Never remove a cover with one side under pressure as the unit will telescope out like a collapsible cup.

**Type II** : units are the condenser and reboiler designs. One side is spiral flow and the other side is in cross flow. These SHEs provide very stable designs



for vacuum condensing and reboiling services. A SHE can be fitted with special mounting connections for reflux-type ventcondenser applications. The vertically mounted SHE directly attaches on the column or tank.

**Type III** : units are a combination of the Type I and Type II where part is in spiral flow and part is in cross flow. This SHE can condense and subcool in a single unit. The unique channel arrangement has been used to provide on-line cleaning, by switching fluid sides to clean the fouling (caused by the fluid that previously flowed there) off the surface. Phosphoric acid coolers use pond water for cooling and both sides foul; water, as you expect, and phosphoric acid deposit crystals. By reversing the flow sides, the water dissolves the acid crystals and the acid clears up the organic fouling. SHEs are also used as oleum coolers, sludge coolers/ heaters, slop oil heaters, and in other services where multipleflow- passage designs have not performed well.

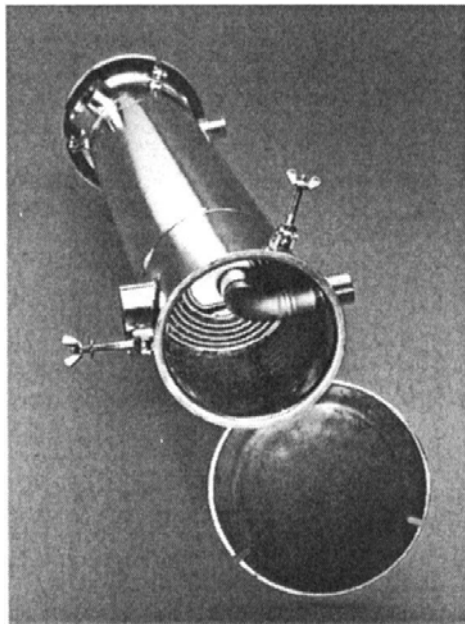


**Fig. 2.3** A compact Spiral Heat Exchanger [10]

### **2.3.3 BRAZED-PLATE-FIN HEAT EXCHANGER**

Brazed-aluminum-plate-fin heat exchangers (or core exchangers or cold boxes) as they are sometimes called, were first manufactured for the aircraft industry during World War II. In 1950, the first tonnage air-separation plant with these compact, lightweight, reversing heat exchangers began producing oxygen for a steel mill. Aluminum-plate fin exchangers are used in the process and gas-separation industries, particularly for services below  $-45^{\circ}\text{C}$ . Core exchangers are made up of a stack of rectangular sheets of aluminum separated by a wavy, usually perforated, aluminum fin. Two ends are sealed off to form a passage. The layers have the wavy fins and sealed ends alternating at  $90^{\circ}$  to each. Aluminum half-pipe-type headers are attached to the open ends to route the fluids into the alternating passages. Fluids usually flow at this same  $90^{\circ}$  angle to each other. Variations in the fin height, number of passages, and the length and width of the prime sheet allow for the core exchanger to match the needs of the intended service. Design conditions range in pressures from full vacuum to 96.5 bar.g and in temperatures from  $-269^{\circ}\text{C}$  to  $200^{\circ}\text{C}$ . This is accomplished meeting the quality standards of most pressure vessel codes.

Applications are varied for this highly efficient, compact exchanger. Mainly it is seen in the cryogenic fluid services of air-separation plants, refrigeration trains like in ethylene plants, and in natural-gas processing plants. Fluids can be all vapor, liquid, condensing, or vaporizing. Multi-fluid exchangers and multi-service cores, that is one exchanger with up to 10 different fluids, are common for this type of product.

Cold boxes are a group of cores assembled into a single structure or module, prepiped for minimum field connections [11].

### **2.3.4 PLATE-FIN TUBULAR EXCHANGERS (PFE)**

These shell and tube exchangers are designed to use a group of tightly spaced plate fins to increase the shellside heat transfer performance as fins do on double-pipe exchangers. In this design, a series of very thin plates (fins), usually of copper or aluminum material, are punched to the same pattern as the tube layout, spaced very close together, and mechanically bonded to the tube. Fin spacing is 315–785 FPM (Fins Per Meter) with 550 FPM most common. The fin thicknesses are 0.24 mm for aluminum and 0.19 mm for copper. Surface-area ratios over bare prime-tube units can be 20:1 to 30:1. The cost of the additional plate-fin material, without a reduction in shell diameter in many cases, and increased fabrication has to be offset by the total reduction of plot space and prime tube-surface area.

The more costly the prime tube or plot space cost, the better the payout for this design. A rectangular tube layout is normally used, no tubes in the window (NTIW). The window area (where no tubes are) of the plate-fins are cut out. This causes a larger shell diameter for a given tube count compared to conventional tubular units. A dome area on top and bottom of the inside of the shell has been created for the fluid to flow along the tube length. In order to exit the unit the fluid must flow across the plate-finned tube bundle with extremely low pressure loss. The units from the outside and from the tubeside appear like any conventional shell and tube exchanger. Two principal applications are rotating equipment oil coolers and compressor inter- and after-coolers. Although seemingly different applications, both rely on the shellside finning to enhance the heat transfer of low heat-transfer characteristic fluids, viscous oils, and gases. By nature of the fluids and their applications, both are clean servicing. The tightly spaced fins would be a maintenance problem otherwise.

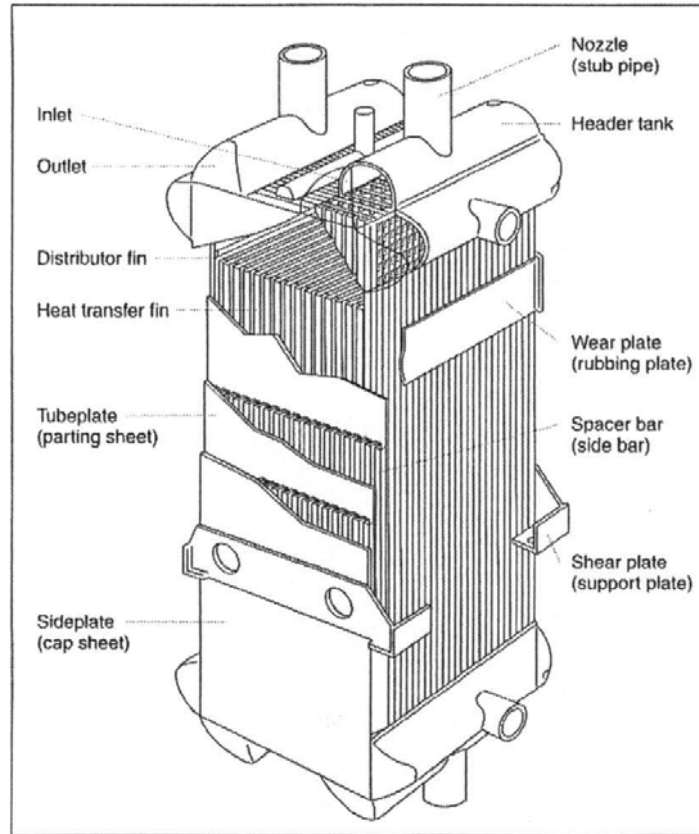


**Fig. 2.4** Basic structure of Plate Fin Heat Exchanger (PFHE) [10]

### 2.3.5 SPIRAL-TUBE EXCHANGERS (STE)

These exchangers are typically a series of stacked helical-coiled tubes connected to manifolds, then inserted into a casing or shell. They have many advantages like spiral-plate designs, such as avoiding differential expansion problems, acceleration effects of the helical flow increasing the heat transfer coefficient, and compactness of plot area. They are typically selected because of their economical design. The most common form has both sides in helical flow patterns, pure countercurrent flow is followed and the LMTD correction factor approaches 1.0. Temperature crosses are possible in single units. Like the spiral-plate unit, different configurations are possible for special applications.

Tube material includes any that can be formed into a coil, but usually copper, copper alloys, and stainless steel are most common. The casing or

shell material can be cast iron, cast steel, cast bronze, fabricated steel, stainless, and other high-alloy materials. Units are available with pressure vessel code conformance. The data provided herein has been supplied by Graham Mfg. for their units called Heliflow. The common Heliflow applications are tank-vent condensers, sample coolers, pump-seal coolers, and steam-jet vacuum condensers. Instant water heaters, glycol/water services, and cryogenic vaporizers use the spiral tube's ability to reduce thermally induced stresses caused in these applications. Many other applications are well suited for spiral tube units but many believe only small surface areas are possible with these units. Graham Mfg. states units are available to 60 m<sup>2</sup>. Their ability to polish the surfaces, double-wall the coil, use finned coil, and insert static mixers, among others configurations in design, make them quite flexible. Tubeside design pressures can be up to 69000 kPa. A cross-flow design on the external surface of the coil is particularly useful in steam-jet ejector condensing service. These Heliflow units, can be made very cost-effective, especially in small units. The main differences, compared to spiral plate, is that the tubeside cannot be cleaned except chemically and that multiple flow passages make tubeside slurry applications (or fouling) impractical.

### **2.3.6 PRINTED CIRCUIT HEAT EXCHANGER**

Heatric is a wholly owned subsidiary of Meggitt PLC and is a manufacturer of Printed Circuit Heat Exchangers for gas processing and petrochemical markets. The major benefits of this technology are:

- Very compact heat exchangers;
- Core design is readily tailored for containment of exceptionally high pressure. Design pressures in excess of 500 bars are feasible;

- The all-metal diffusion bonded and welded construction of PCHEs minimise design temperature constraints. Materials such as austenitic stainless steels are suitable for temperatures ranging from cryogenic to 800°C.
- High efficiency heat exchanger;
- Used to very harsh working conditions (off-shore applications).

PCHEs are constructed from flat metal plates into which fluid flow channels are chemically milled. The chemical milling technique is similar to that employed for etching electrical printed circuits, and hence is capable of producing fluid circuits of unlimited variety and complexity. The channel may be straight or wavy. The milled plates are then stacked and diffusion bonded together to form strong, compact, all-metal heat exchange cores (see figure 3). The diffusion bonding is a "solid-state joining" process entailing pressing metal surfaces together at temperatures below the melting point, thereby promoting grain growth between the surfaces. Under carefully controlled conditions, diffusion bonded joints reach parent metal strength, and stacks of milled plates are converted into solid blocks containing the fluid flow passages. The blocks are then welded together to form the complete heat exchange core for the thermal duty. Finally, fluid headers and nozzles are welded to the core in order to direct the fluids to the appropriate sets of passages. No gaskets or brazing material – potential sources of leakage, fluid incompatibility and temperature limitations - are required for exchanger assembly. Classically, the hydraulic diameters are less than 1 mm which leads to laminar flow regimes on both sides. Moreover, the channels can be shaped (straight or wavy) in order to generate turbulence inside. This technology seems to be very promising in terms of high pressure / temperature resistance and compactness. Furthermore, the diffusion bounding process leads to a single-metal heat exchanger, without secondary-metal supply. [12]

## 2.4 Design for Some Types of Compact Heat Exchangers

### 2.4.1 Design of Gasketed-Plate Exchangers (G. PHE)

Standard channel-plate designs, unique to each manufacturer, are developed with limited modifications of each plates' corrugation depths and included angles. Manufacturers combine their different style plates to custom-fit each service. Due to the possible combinations, it is impossible to present a way to exactly size PHEs. However, it is possible to estimate areas for new units and to predict performance of existing units with different conditions (chevron-type channel plates are presented). The fixed length and limited corrugation included angles on channel plates makes the NTU method of sizing practical. (Waterlike fluids are assumed for the following examples).

$$NTU = (\Delta t \text{ of either side} / LMTD)$$

Most plates have NTU values of 0.5 to 4.0, with 2.0 to 3.0 as the most common, (multipass shell and tube exchangers are typically less than 0.75). The more closely the fluid profile matches that of the channel plate, the smaller the required surface area. Attempting to increase the service NTU beyond the plate's NTU capability causes over surfacing (inefficiency).

True sizing from scratch is impractical since a pressure balance on a channel-to-channel basis, from channel closest to inlet to furthest, must be achieved and when mixed plate angles are used; this is quite a challenge. Computer sizing is not just a benefit, it is a necessity for supplier's selection. Averaging methods are recommended to perform any sizing calculations [13].

There are the following equations for plate heat transfer.

$$Nu = \frac{hDe}{k} = 0.28 * (Re)^{0.65} * (Pr)^{0.4} \quad \dots (2.1)$$

where  $De = 2 \times$  depth of single-plate corrugation

$$G = \frac{W}{N_p * w * De} \quad \dots (2.2)$$

Width of the plate ( $w$ ) is measured from inside to inside of the channel gasket. If not available, use the tear-sheet drawing width and subtract two times the bolt diameter and subtract another 50 mm. For depth of corrugation ask supplier, or take the compressed plate pack dimension, divide by the number of plates and subtract the plate thickness from the result. The number of passages ( $N_p$ ) is the number of plates minus 1 then divided by 2.

Typical overall coefficients to start a rough sizing are as below. Use these in conjunction with the NTU calculated for the process. The closer the NTU matches the plate (say between 2.0 and 3.0), the higher the range of listed coefficients can be used. The narrower (smaller) the depth of corrugation, the higher the coefficient (and pressure drop), but also the lower the ability to carry through any particulate.

Water-water 5700–7400 W/(m<sup>2</sup> °C)

Steam-water 5700–7400 W/(m<sup>2</sup> °C)

Glycol/Glycol 2300–4000 W/(m<sup>2</sup> °C)

Amine/Amine 3400–5000 W/(m<sup>2</sup> °C)

Crude/Emulsion 400–1700 W/(m<sup>2</sup> °C)

Pressure drops typically can match conventional tubular exchangers and can be calculated as follows:

$$\Delta P = \frac{2fG^2L}{g\rho De} \quad \dots (2.3)$$

$$\text{where } f = 2.5\left(\frac{GDe}{\mu}\right)^{-0.3} \quad \dots (2.4)$$

$g$  = gravitational constant



Fouling factors are typically 1/10 of TEMA values or a percent over surfacing of 10–20 percent is used [14].

LMTD is calculated like a 1 pass-1 pass shell and tube with no F correction factor required in most cases.

Overall coefficients are determined like shell and tube exchangers; that is, sum all the resistances, then invert. The resistances include the hot-side coefficient, the cold-side coefficient, the fouling factor (usually only a total value not individual values per fluid side) and the wall resistance.

## 2.4.2 Design of Spiral – Plate Heat Exchanger

The provided formulae for heat-transfer and pressure drop calculations. Spacings are from 6.35 to 31.75 mm (in 6.35 mm increments) with 9.5 mm the most common. Stud densities are 60 × 60 to 110 × 110 mm, the former the most common. The width (measured to the spiral flow passage), is from 150 to 2500 mm (in 150 mm increments). By varying the spacing and the width, separately for each fluid, velocities can be maintained at optimum rates to reduce fouling tendencies or utilize the allowable pressure drop most effectively. Diameters can reach 1500 mm. The total surface areas exceed 465 sqm. Materials that work harder are not suitable for spirals since hot-forming is not possible and heat treatment after forming is impractical.

$$Nu = \frac{HDe}{k} = 0.0315(Re)^{0.8} (Pr)^{0.25} \left(\frac{\mu}{\mu_w}\right)^{0.17} \quad \dots (2.5)$$

where  $De = 2 \times \text{spacing}$

Flow area = width × spacing

$$\Delta P = \frac{LV^2 \rho}{1.705E - 03} * 1.45 \quad (1.45 \text{ for } 60 \times 60 \text{ mm studs}) \quad \dots (2.6)$$

LMTD and overall coefficient are calculated like in PHE section above. [15]

### **2.4.3 Design of Plate-Fin Tubular Exchanger**

The economics usually work out in the favor of gas coolers when the centrifugal machine's flow rate reaches about 5000 scfm. The pressure loss can be kept to 7.0 kPa in most cases. When the ratio of  $A_t h_t$  to  $A_s h_s$  is 20:1, is another point to consider these plate-fin designs. Vibration is practically impossible with this design, and uses in reciprocating compressors are possible due to this.

Marine and hydraulic-oil coolers use these characteristics to enhance the coefficient of otherwise poorly performing fluids. The higher metallurgies in marine applications like 90/10 Cu-Ni afford the higher cost of plate-fin design to be offset by the less amount of alloy material being used. On small hydraulic coolers, these fins usually allow one to two size smaller coolers for the package and save skid space and initial cost.

### **2.4.4 Design of Spiral-Tube Exchangers**

The fluid flow is similar to the spiral-plate exchangers, but through parallel tube passages. Graham Mfg. has a liquid-liquid sizing pamphlet available from their local distributor.

The tubeside fluid must be clean or at least chemically cleanable. With a large number of tubes in the coil, cleaning of inside surfaces is not totally reliable. Fluids that attack stressed materials such as chlorides should be reviewed as to proper coil-material selection. Fluids that contain solids can be a problem due to erosion of relatively thin coil materials unlike the thick plates in spiral-plate units and multiple, parallel, fluid passages compared to a single passage in spiral-plate units [16].

## 2.4.5 Design of Printed Circuit Heat Exchanger

For the thermal-hydraulic correlations, one needs first to define the flow regime, classically based on the

Reynolds number  $Re = (\rho U D_H / \mu)$  where  $U$  bulk flow velocity (m/s),  $\rho$  the fluid density ( $\text{kg/m}^3$ ),  $\mu$  dynamic viscosity (Pa.s) and  $D_H$  the hydraulic diameter given by  $D_H = (4 S / P)$  with  $S$  the cross section ( $\text{m}^2$ ) and  $P$  the wetted perimeter (m). Depending on the Reynolds number, three various flow regimes exist: laminar ( $Re \leq 2300$ ), transitional ( $2300 \leq Re \leq 10000$ ) or turbulent ( $Re \geq 10000$ ). Pressure drops  $\Delta P$  are computed with

$$\Delta P = \Lambda(L / D_H)(\rho U^2 / 2) \quad \dots (2.7)$$

Where  $L$  is the length of the duct (m) and  $\Lambda$  is the Darcy factor.

**For a straight rectangular channel**, the following correlations allow to estimate the Darcy coefficient:

- $Re \leq 2300$  : Shah and Bhatti [17] proposed for  $0 < \alpha^* < 1$ ,  $\alpha^* = 2b/2a$  with  $2b$  the channel height (m) and  $2a$  the channel width (m).

$$\Lambda = \frac{[96(1 - 1.3553\alpha^* + 1.9467\alpha^{*2} - 1.7012\alpha^{*3} + 0.9564\alpha^{*4} - 0.2537\alpha^{*5})]}{Re} \quad (2.8)$$

- $5000 \leq Re \leq 10^7$  : Shah and Bhatti proposed the following correlation for  $0 < \alpha^* < 1$

$$\Lambda = 4(1.0875 - 0.1125\alpha^*)f_c \quad \dots (2.9)$$

where  $f_c = [1.7372 \ln[\frac{Re}{1.964 \ln Re - 3.8215}]]^{-2} \quad \dots (2.10)$

For the thermal point of view ,

- $0 \leq Re \leq 2300$  In the laminar flow regime, the heat transfer coefficient is a function of the heating conditions (fixed wall temperature or fixed heat flux).
- $2300 \leq Re \leq 10^6$  : The well-known Colburn correlation could be used :

$$Nu = 0.023 Re^{0.8} Pr^{1/3} \quad \dots (2.11)$$

**For a wavy channel** (herringbone pattern), no general correlation exists. However, Hesselgreaves [10] proposed a relation which takes into account the wavy geometrical parameters  $b$ , the channel width,  $p$  the wavy pitch length and  $w$  the wave height.

The available correlations according to the flow regime are the following:

- $10^4 \leq \text{Re} \leq 10^5$  :

$$f = 4.8 \text{Re}^{-0.36} \left(\frac{2b}{p}\right)^{1.5} \quad \dots (2.12)$$

$$j = 0.4 \text{Re}^{-0.36} \left(\frac{2b}{p}\right)^{0.75} \quad \dots (2.13)$$

- $600 \leq \text{Re} \leq 2300$  :

$$j = 0.4 \text{Re}^{-0.4} \left(\frac{2b}{p}\right)^{0.75} \quad \dots (2.14)$$

$$f = 5j \quad \dots (2.15)$$

According to the author, this relation predicts the experimental data quite well for  $w/p = 0.25$ .

## **Basic Aspects of Compactness [10]**

### **Geometrical aspects**

The fundamental parameter describing compactness is the hydraulic diameter  $D_H$ , defined as

$$D_H = \frac{4A_c L}{A_s} \quad \dots (2.16)$$

For some types of surface the flow area  $A_c$  varies with flow length, so for these an alternative definition is

$$D_H = \frac{4V_s}{A_s} \quad \dots (2.17)$$

where  $V_s$  is the enclosed (wetted) volume.

This second definition enables us to link hydraulic diameter to the surface area density  $\beta$ , which is  $A_s/V$ , also often quoted as a measure of

compactness. Here, the overall surface volume  $V$  is related to the surface porosity  $\sigma$  by :

$$\sigma = \frac{V_s}{V} \quad \dots (2.18)$$

so that the surface area density  $\beta$  is

$$\beta = \frac{A_s}{V} = \frac{4\sigma}{D_H} \quad \dots (2.19)$$

A commonly accepted lower threshold value for  $\beta$  is  $300 \text{ m}^2/\text{m}^3$ , which for a typical porosity of 0.75 gives a hydraulic diameter of about 10 mm . For tubes this represents the inside tube diameter, and for parallel plates it represents a plate spacing of 5 mm - typical of the plate and frame generation of exchangers. An informative figure given by Shah [17] shows the 'spread' of values and representative surfaces - mechanical and natural.

It should be noted at this point that the porosity affects the actual value of surface density, independently of the active surface. In Figure 2.5, the value of 0.83 is chosen which is typical of high performance plate- fin surfaces with aluminum or copper fins. As hydraulic diameter is progressively reduced, it is less easy to maintain such a high value, especially for process exchangers. This is for two reasons, both associated with the effective fin thickness. Firstly, for high temperature and high pressure containment, stainless steel or similar materials are necessary for construction, and diffusion bonding is the preferred bonding technique. This in turn requires significantly higher fin thicknesses to contain the pressure. Secondly, the lower material thermal conductivity calls for higher thicknesses to maintain an adequate fin efficiency and surface effectiveness. Thus typical values for porosity for diffusion bonded exchangers are from 0.5 to 0.6, so having a strong effect on surface density and exchanger weight. Brazed stainless steel plate-fin exchangers have intermediate porosities of typically 0.6 to 0.7.

## 2.5 Heat Transfer Aspects of Compactness

The heat transfer coefficient  $\alpha$  is usually expressed, in compact surface terminology, in terms of the dimensionless  $j$ , or Colburn, factor by the definition

$$j = \frac{Nu}{Re Pr^{1/3}} = St Pr^{2/3} \quad \dots (2.20)$$

where  $Nu$  = Nusselt number  $Nu = \frac{\alpha D_H}{\lambda}$

and  $St$  = Stanton number  $St = \frac{\alpha}{GC_p}$

Thus  $\alpha$  is non-dimensionalised in terms of the mass velocity  $G$ : for a fixed  $G$ ,  $j$  is proportional to  $\alpha$ .

For a single side, a specified heat load,  $q^\bullet$ , is given by the heat transfer and rate equations

$$q^\bullet = \alpha A_s \Delta T_m = m^\bullet C_p (T_2 - T_1) \quad \dots (2.21)$$

neglecting for convenience the influences of wall resistance and surface efficiency on  $\alpha$ . The first part of equation 2.21 can be written, using equation 2.19

$$q^\bullet = \alpha \frac{4\sigma V}{D_H} \Delta T \quad \dots (2.22)$$

Thus for a specified heat load  $q^\bullet$ , to reduce the volume  $V$  means that we must increase the ratio  $\alpha / D_H$ . The choice therefore is to increase heat transfer coefficient or to decrease hydraulic diameter (increase compactness), or both. We will make the distinction that enhancement implies increasing  $\alpha$  with no change of compactness.

In fully- developed laminar flow, the Nusselt number is constant, that is, importantly, independent of Reynolds number, giving

$$\alpha = \frac{Nu \lambda}{D_H} \quad \dots (2.23)$$

Substituting this into equation 2.22 gives

$$q^{\bullet} = \frac{4\sigma V Nu \lambda \Delta T}{D_H^2} \quad \dots (2.24)$$

Hence for a given  $q^{\bullet}$  and temperature difference, the exchanger volume required is proportional to the inverse square of the hydraulic diameter, for laminar flows. This volume requirement is unchanged whatever the specified pressure drop, as is shown later (although the shape does change).

The situation for flows other than fully- developed laminar is more complex, needing compatibility of both thermal and pressure drop requirements. It is shown that the thermal requirement (the heat load  $q^{\bullet}$ ) is linked to the surface performance parameter  $j$  by

$$j = \frac{A_c}{A_s} Pr^{2/3} N \quad \dots (2.25)$$

where  $N = NTU$  (Number of Thermal Units) for the side

$$= (T_2 - T_1) / \Delta T_m \text{ for this case.}$$

Alternatively, in terms of the hydraulic diameter and flow length,

$$j = \frac{D_H}{4L} Pr^{2/3} N \quad \dots (2.26)$$

For given conditions the product  $Pr^{2/3} N$  is fixed, so the required  $j$  factor is proportional to the aspect ratio  $D_H / L$  of the surface. Thus from the thermal requirement, the flow length element of size and shape is reduced directly by reducing hydraulic diameter and maintaining the  $j$  factor. Put another way, the same heat transfer coefficient is obtained if  $G$  and the ratio  $dh/L$  are fixed. The latter condition also implies that the surface area to flow area ratio is fixed, through equation 2.16.

The equivalent expression to equation 2.24 for a surface described by a  $j$  factor is

$$q^{\bullet} = \frac{4\sigma V j Re Pr^{1/3} \lambda \Delta T}{D_H^2} \quad \dots (2.27)$$

Here, although the superficial square law relationship with hydraulic diameter is retained, the hydraulic diameter affects the Reynolds number; this in turn influences the  $j$  factor. The Reynolds number is constrained in addition by the mass velocity, which depends on pressure drop, unlike the fully-developed laminar case.

The required pressure drop is thus a significant factor in the shape and size of exchangers. Neglecting, for many practical exchangers, the relatively small contributions of entry and exit losses and flow acceleration, the pressure drop  $\Delta P$  of fluid through a surface is given by

$$\Delta P = \frac{1}{2} \rho u^2 \frac{4L}{D_H} f \quad \dots (2.28)$$

$f$  being the Fanning friction factor.

Relating the mean velocity  $u$  to the mass flow rate, we have

$$\frac{2\rho\Delta P}{m \cdot^2} = f \frac{4L}{D_H A_c} = \text{constant for given conditions.} \quad \dots (2.29)$$

We can now combine the thermal and pressure drop requirements in the core mass velocity equation, after London [18] , which can now be derived from equations 2.26 and 2.29:

$$\frac{2\rho\Delta P}{m \cdot^2} = f \frac{\text{Pr}^{2/3} N}{j A_c^2} \quad \dots (2.30)$$

and

$$\frac{G^2}{2\rho\Delta P} = \frac{j/f}{\text{Pr}^{2/3} N} \quad \dots (2.31)$$

For given conditions of  $\text{Pr}$ ,  $N$ ,  $\rho$  and  $\Delta P$ , it is clear that  $G$  is only a function of  $j/f$ , and most importantly is independent of hydraulic diameter of the surface. As pointed out by London,  $j/f$  is only a weak function of Reynolds number, being of the order of 0.2 to 0.3 for most compact surfaces.



Thus  $G$ , and hence flow area, can be closely estimated from the design specification.

Examination of the pressure drop and thermal requirements together thus shows that the mass velocity  $G$  and hence the flow area are closely circumscribed by the specification. If the aspect ratio of the surface (not the exchanger),  $D_H/L$ , is maintained, then both the heat transfer coefficient and the surface area are also the same between two cases, hence giving the same performance.

We have now established the basic elements of the effect of the surface on the thermal design of a non-laminar flow exchanger, with the normal (but not the invariable) specification of both heat load and pressure drop. These are:

- that flow length decreases as hydraulic diameter decreases
- that flow area is largely independent of hydraulic diameter

The straightforward implication of this is that exchanger cores are changed in their aspect ratio as they are made more compact, whilst their internal surfaces maintain a constant or nearly constant ratio  $D_H/L$ . The heat transfer coefficient and surface area change according to the change in consequent Reynolds number.

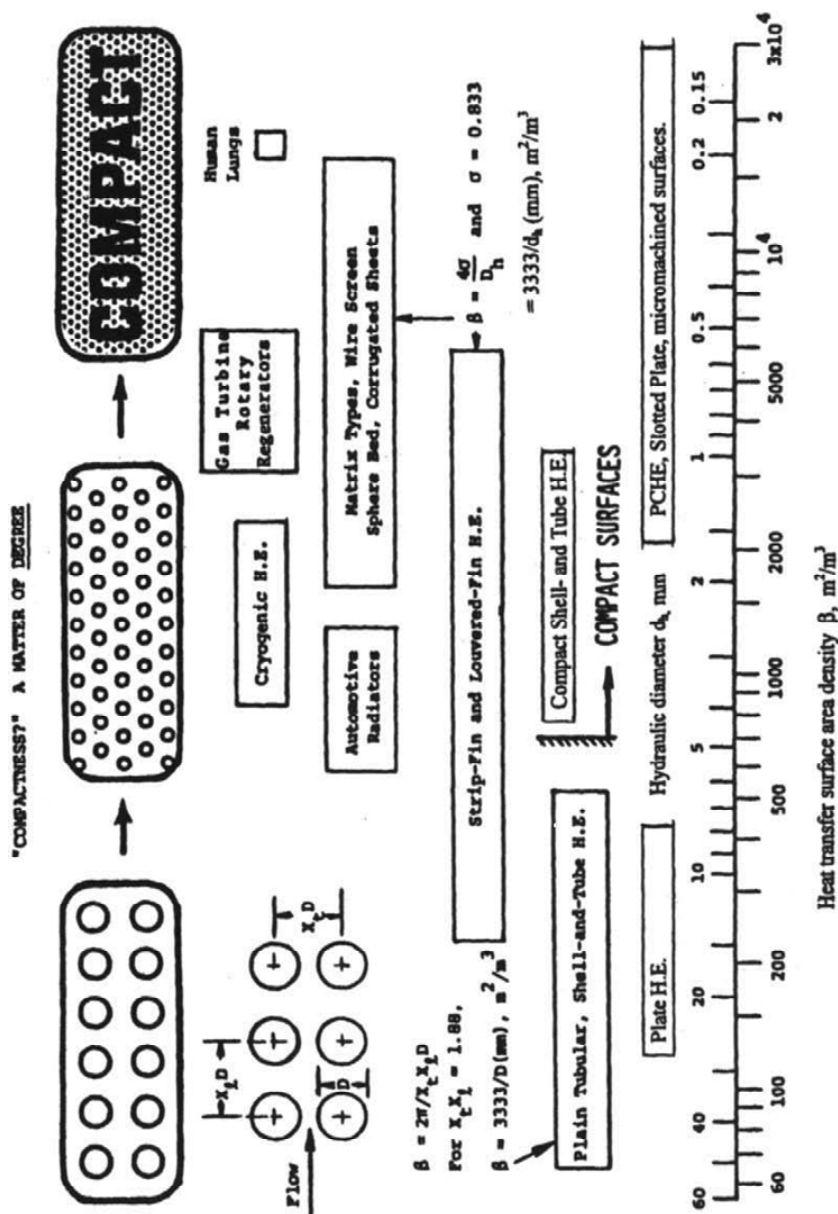


Fig . 2.5 Overview of compact heat transfer surfaces, adapted from Shah [17]

## 2.6 Effectiveness – NTU Method

The LMTD approach to heat exchanger analysis is useful when the inlet and outlet temperatures are known or are easily determined. The LMTD is then easily calculated, and the heat flow, surface area, or overall heat transfer coefficient may be determined. When the inlet or exit temperatures

are to be evaluated for a given heat exchanger, the analysis frequently involves an iterative procedure because of the logarithmic function in the LMTD . In these cases the analysis is performed more easily by utilizing a method based on the effectiveness of heat exchanger in transferring a given amount of heat. The effectiveness method also offers many advantages for analysis of problems in which a comparison between various types of heat exchangers must be made for purpose of selecting the type best suited to accomplish a particular heat-transfer objective [19].

The heat exchanger effectiveness can be defined as

Effectiveness =  $\varepsilon$  = (actual heat transfer/ maximum possible heat transfer)

The actual heat transfer may be computed by calculating either the energy lost by the hot fluid or the energy gained by the cold fluid.

## 2.7 Functional Form of the Overall Heat Transfer Coefficient

The inner and outer heat transfer coefficients are usually combined into a single overall transfer coefficient to calculate the heat rate. Although there are a number of ways in which this can be done, the common approach is to use a particular functional form in which the reciprocal of the overall transfer coefficients an additive function of two independent expressions, one dependent on the inner and another on the outer mass flow rates. The explicit form, known as the thermal resistance equation in which each quantity can be thought to be a thermal resistance on either side of the heat exchanger. The overall thermal resistance of a heat exchanger can be divided up into four major parts: the water side, tube conduction, contact conduction (between the tube and fin), and air side thermal resistance.

$$\frac{1}{UA_o} = R_o = R_w + R_{t,cond} + R_{c,cond} + R_A = \frac{1}{h_i A_i} + \frac{\delta_t}{k_t A_t} + \frac{1}{h_c A_t} + \frac{1}{\eta_o h_o A_o} \dots (2.32a)$$

The conduction resistance through the tube wall,  $R_{t,cond}$ , was calculated to be less than 0.5% of the total resistance in all cases. The contact conduction

resistance,  $R_{c,cond}$ , between the tube and the collar of the fin is a source of uncertainty. Wang [20] states that “in practice it is very hard to accurately predict the contact conductance, and most of the published works on the air side performance absorbed contact resistance into the airside performance.” The work of Sheffield et al. [21] gave a range of thermal contact conductance of 10,607 – 30,828 W m<sup>-2</sup> K<sup>-1</sup> [1750 – 5400 Btu/ft<sup>2</sup>-hr-R] for a similar fin geometry ( $X_t = 25.4$  mm [1 in.],  $X_l = 22$  mm [0.866 in.],  $D_o = 9.52$  mm [0.375 in.], and full fin collar). Based on this range, the contact conductance accounts for 3% - 18% of the total thermal resistance in the coils tested. Both the tube conduction resistance and the contact conduction resistance were absorbed into the airside thermal resistance.

Solving Equation 4.1 for the air side heat transfer coefficient produces.

$$h_o = \frac{1}{\eta_o A_o} \left[ \frac{1}{UA_o} + \frac{1}{h_i A_i} \right]^{-1} \quad \dots(2.32b)$$

The air side fin efficiency  $\eta_o$ , is calculated using the Zeller hexagonal fin approximation. This approximation was used for both the plain and louvered fins, although it is known that the louvers impede radial heat flow from the tube, resulting in an over estimate of the fin efficiency for louvered fins. The  $UA_o$  term is calculated using the Variable Air Test; the  $h_i$  term is calculated using the Wilson Test. The main advantage of this functional form, from an experimental standpoint, is that if one of the resistances is zero or known a priori, then the value of the other is immediately determined. On the other hand, the summing function implies that the heat transfer coefficient on one side does not depend on the mass flow rate of the other side and hence assumes the existence of a wall temperature separating the two fluids. For unidirectional parallel- and counter-flow arrangements this local wall temperature, although sometimes unknown, is physically well-defined. In most heat exchanger configurations, such as the fin-tube type, however, it is

well-known not to be the case. The inclusion of a tube-arrangement and a set of fins makes it very difficult not only to measure the temperature at the wall but moreover to specify where it should be measured. Furthermore, property variations with temperature break the assumption of independence of the transfer coefficients. Nevertheless, it is possible to define a hypothetical local wall temperature that allows us to still use the aforementioned approach to compute the heat rate. In such a case, although the coefficients of heat transfer remain coupled, it is possible to find them in a least squares sense. The hypothetical wall temperature will then be defined such that it fits the experimental data the best. The accurate determination of both coefficients is a challenging problem [22].

## 2.8 Previous Work

Despite the importance of fin-and-tube heat exchangers, very little experimental work of general use has been reported. The most extensive investigation in this area has been that of **Shepherd (1956)** [23], who tested a total of 38 different single-row coils. The information is presented in the form of average air-side transfer coefficients and transfer rates. These transfer coefficients were evaluated without the fin efficiency being taken into account. In addition, there is uncertainty in his data reduction procedure. The method used to determine the air-side heat transfer coefficients was to measure the overall thermal resistance and then to extrapolate it for the limit of zero water-side resistance.

A different approach for the calculation of the heat transfer coefficient was that used by **Saboya and Sparrow (1974)** [24]. In their work the analogy between heat and mass transfer was used to obtain local and average transfer coefficients. The mass transfer measurements were performed using the naphthalene sublimation technique. These experiments thus correspond to

heat transfer from isothermal fins, that is fins with efficiency  $\eta = 1$ .

A paper by **Rich (1973)** [25], analyzed the effect of fin spacing on the heat transfer performance on plate fin-and-tube heat exchangers. In the experiment, the fin spacing was varied from zero to 21 fins per inch. In a further paper (Rich, 1975), the effect of number of tube rows was studied. The experiment was made for six plate fin-and-tube heat exchangers in which the primary physical variable was the flow depth, which varied from one to six rows. The heat transfer coefficient was presented using the Colburn j-factor. It is important to mention that the test coils in the experiments were of all-copper construction, and in the data reduction, a fixed average value of metal resistance was used provided that it varies only slightly with the air resistance.

**McQuiston (1981)** [26] used data from another worker and from his own experiments to obtain the first correlation for smooth-plate fin and tube coils. He considered the effects of rows, fin pitch, and other geometrical parameters and generalized a heat transfer correlation useful for dry coils.

The heat transfer correlation was developed in two steps. The first step developed a correlation for finned-tube geometries having four tube rows

$$j_4 = 0.0014 + 0.2168Re_a^{-0.4} \left( \frac{A}{A_t} \right)^{-0.15} \quad (2.33)$$

Then a multiplier was considered to account for the effect of the number of rows

$$\frac{j_N}{j_4} = \frac{1 - 180NRe_{a,L}^{-1.2}}{1 - 5120Re_{a,L}^{-1.2}} \quad (2.34)$$

where  $500 < Re_a < 24700$ .

**Webb (1986)** [27] complemented the data from another worker with data for bundles of finned tubes. He developed his own regression technique to obtain another correlation for plate finned-tube heat exchangers with plain

fins. This new correlation predicts the four row j-factor

$$j_4 = 0.14Re_a^{-0.328} \left(\frac{S_t}{S_l}\right)^{-0.502} \left(\frac{s}{D}\right)^{0.0312} \quad (2.35)$$

and then corrects it for the effect of different number of rows

$$\frac{j_N}{j_4} = 0.991[2.24Re^{-0.092} \left(\frac{N}{4}\right)^{-0.031} J^{0.0607(4-N)}] \quad (2.36)$$

where  $2400 < Re_a < 24700$ . The range of dimensionless variables for equations (2.2) and (2.4) are  $1.97 < St/D < 2.55$ ;  $1.70 < S_l/D < 2.58$ ;  $0.08 < s/D < 0.64$ ;  $1 < N < 8$  or more.

**Yan and Lin (1999)** [28] stated that many simplified models for heat exchangers have been proposed. An analytical approach for predicting the air-side performance of a single-phase heat exchanger with louvered fins was developed by Sahnoun and Webb (1992). Their model predicted heat transfer coefficients with errors of as much as 25%. For calculating the air-side heat transfer in heat exchangers under condensing conditions an analytic method has been described by Ramadhyani (1998). Recently, Srinivasan and Shah (1997) examined condensation phenomena occurring in compact heat exchangers.

Other attempts to analyze transport phenomena in the air-side, within the fin-tube passages (Kushida et al., 1986; Bastani et al., 1992; Torikoshi et al., 1994), and in the water-side, inside the tube bends (Goering et al., 1997), have been carried out with CFD techniques assuming isothermal fins. Ranganayakulu and Seetharamu (1999) performed a steady state simulation of a single-phase heat exchanger using finite elements. Their analysis included the effect of one-dimensional heat conduction at the wall, nonuniformity in the inlet fluid flow, and a few different models of temperature distributions. For condensing heat exchangers very few numerical studies of the thermal-

hydraulic characteristics have been carried out. Wagner (1998) developed a moving grid algorithm to analyze the change of phase in a counter-flow heat exchanger, whereas a three-dimensional numerical study of heat transfer under dry and wet conditions was reported by Jang et al. (1998). Unfortunately, the common thread in the aforementioned studies is the inclusion of assumptions and situations that are far from being compatible with the phenomena that exist in heat exchangers. A large amount of experimental information about transport phenomena in single-phase , cooling, and evaporator heat exchangers are reported in the open literature (Webb, 1980; Kaka,c et al., 1981; Kays and London, 1984; Shah et al., 1990). For instance, Beecher and Fagan (1987) determined performance data for single-phase finned-tube heat exchangers; Jacobi and Goldschmidt (1990) characterized, experimentally, heat and mass transfer performance of a condensing heat exchanger. Similar studies were also examined by McQuiston (1978a), Mirth and Ramadhyani (1995), and Yan and Sheen (2000). Thermal performance data for evaporators have been developed by Panchal and Rabas (1993). These findings are all based on the experimentally determined overall, air-side and water-side heat transfer coefficients.

A few studies have been carried out to find correlations for the performance of compact heat exchangers. The most representative examples are those for single-phase operating conditions (Gray and Webb, 1986), for heat exchangers operating under wet conditions (McQuiston, 1978b), and for evaporators (Kandlikar, 1991). Some applications of correlations to the modeling of condensers and evaporators are those reported by Kandlikar (1990), Srinivasan and Shah (1997), and Corberan and Melon (1998)., among others.

The determination of the inner heat transfer coefficient (water-side) is a problem which has received little attention in papers related to fin-tube heat



exchangers.

In the vast majority of papers related to fin-tube heat exchangers, simple straight-tube correlations are assumed for the water side circuit, thus leading to inaccurate results in the determination of the inner heat transfer coefficient, especially at low Reynolds numbers.

A paper of **Mirth et al.(1993)** [29] revealed that cooling coils operating at low water-side Reynolds numbers do not perform as predicted by manufacturer's software. Based upon this observation, they suggested that further research is needed to obtain a suitable prediction for coils operating at low Reynolds numbers. This need is aggravated because in the laminar flow region the inner heat transfer coefficient is even more important in the determination of the overall heat transfer coefficient than for turbulent flows.

On the other hand, it should be noted here that, even though much experimental data and correlations are now available in the literature on fin-tube heat exchangers, these data largely emphasize the air- or gas-side heat transfer characteristics.

## **Chapter Three**

### **Experimental Work**

#### **3.1 Introduction**

The experiments were carried out in a test facility specifically designed and constructed for the purpose. A schematic of this facility is shown in Fig 3.1. Photographs of this test system in different views are shown in Fig. 3.2 and 3.3.

#### **3.2 Components of Test System**

- 1- Water bath: Memmert type, was used to heat the water entering the heat exchanger with a constant temperature of 60°C
- 2- Compact heat exchanger: the main part in the system was made of copper and its dimensions are 20 x 19 x 5cm, number of pipes is 18 outside diameter of the pipe is 0.45 cm , and has 7 fins/cm with fin thickness of 0.5 mm.
- 3- Cooling Fan: Flat motor DC 12 V fan, was used to cool the heat exchanger
- 4- Water pump: Akad type, Iraq with 220V, power of 80W, volumetric flow rate of 0.5 m<sup>3</sup>/hr at head 1.4 m, was used to pump water from water bath to the heat exchanger.
- 5- Power supply: HP type DC 0-40V, 0-5A, using to give the power to the fan with three different voltages which cause three different air flow rates.
- 6- Rubber tubes: was used to transport water to/from heat exchanger.
- 7- Thermometer: to measure the temperature of in/out water and air.

#### **3.3 Test Measuring Parameters and Procedure**

The measured parameters and their ranges during test were listed below:

- Water inlet temperature  $T_{w,in}$ : 60°C .
- Water outlet temperature  $T_{w,out}$  : 51.0 - 57.5 °C .

- Air inlet temperature  $T_{a,in} : 34 \text{ }^\circ\text{C}$  .
- Air outlet temperature  $T_{a,out} : 39.5 - 45.2 \text{ }^\circ\text{C}$  .
- Water flow rate  $Q_w: 1.4 \times 10^{-4} \text{ m}^3/\text{s}$  .
- Air flow rate  $Q_a: 3.5 \times 10^{-2} - 4.5 \times 10^{-2} \text{ m}^3/\text{s}$  .

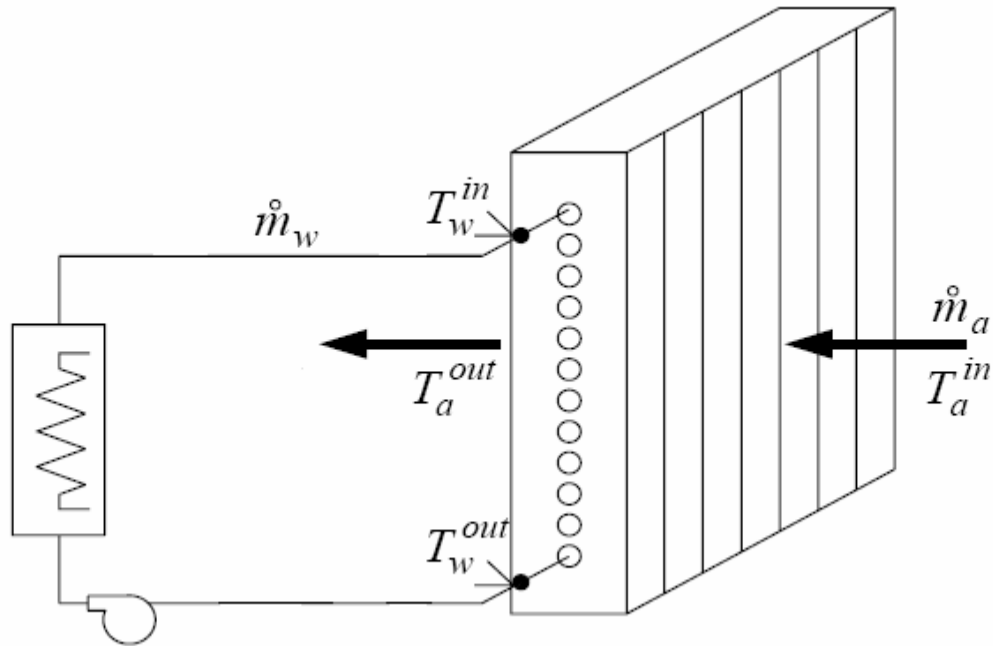


Fig. 3.1 Schematic diagram of the system.

Laboratory experiments have been performed to obtain dynamical response data for the heat exchanger. Tests were carried out with a constant water volumetric flow rate value of  $1.4 \times 10^{-4} \text{ m}^3/\text{s}$  , and constant values for both water and air inlet temperature of  $60^\circ\text{C}$  and  $34 \text{ }^\circ\text{C}$  . The air inlet temperature is the same as the room temperature. For a fixed water flow rate , the air flow rate was changed by changing the voltage supplied to the fan using the power supply and so, the fan's velocity will change .

The outlet temperatures of water and air were measured with every change, using the thermometer, which was fixed near the fan to measure the outlet air

temperature, and the other thermometer was fixed in the end of the tube to measure the outlet water temperature and the heat transfer performance was studied with the change of air flow rate. The water flow rate was measured by draining water from the outlet of the tube out of the heat exchanger into a graduated cylinder and measuring the water volume in a certain time period.



**Fig.3.2a** View of the system(View A).



**Fig.3.2b** View of the system(View B).

### 3.4 Test results

#### 3.4.1 First test

The first test is done at the following conditions tabulated in Table 3.1

**Table 3.1** specifications of first test.

Fluid type	Volumetric flow rate m <sup>3</sup> /s	Mass flow rate Kg/s	Inlet temperature in °C
Water	0.00014	0.1369	60
Air	0.035	0.4060	34

The results of the first test are tabulated in table 3-2

**Table 3.2** Results of the first test.

Time(min)	$T_{w,out}(^{\circ}C)$	$T_{a,out}(^{\circ}C)$
0	60	34
0.5	59	36
1.0	58.5	39
1.5	57.8	39.7
2.0	57	40
2.5	56.5	40.2
3.0	56	40.5
3.5	55.8	40.8
4.0	55.4	40.8
4.5	55	41
5.0	55	41
7.0	55	41

**3.4.2 Second test**

The second test is done at the following conditions tabulated in Table 3.3

**Table 3.3** Specifications of second test.

Fluid type	Volumetric flow rate $m^3/s$	Mass flow rate $Kg/s$	Inlet temperature in $^{\circ}C$
Water	0.00014	0.1369	60
Air	0.041	0.4618	34

The results of the second test are tabulated in table 3.4

**Table 3.4** Results of the second test.

Time(min)	$T_{w,out}(^{\circ}C)$	$T_{a,out}(^{\circ}C)$
0	60	34
0.5	58.5	37
1.0	57	40
1.5	56	40.5
2.0	55	40.8
2.5	54.5	41.2
3.0	54	41.6
3.5	53.8	41.8
4.0	53.5	42
4.5	53.5	42
5.0	53.5	42
7.0	53.5	42

### 3.4.3 Third test

The Third test is done at the following conditions tabulated in Table 3.5

**Table 3.5** specifications of third test.

Fluid type	Volumetric flow rate m <sup>3</sup> /s	Mass flow rate Kg/s	Inlet temperature in °C
Water	0.00014	0.1369	60
Air	0.045	0.5115	34

The results of the second test are tabulated in table 3.6

Table 3.6 Results of the third test

Time(min)	T <sub>w,out</sub> (°C )	T <sub>a,out</sub> (°C )
0	60	34
0.5	58.5	38
1.0	57	41
1.5	56	41.5
2.0	55	42
2.5	54	42.3
3.0	53	43
3.5	52	43.5
4.0	51.5	44
4.5	51	44
5.0	51	44

### 3.5 Control of the Heat Exchanger (Unsteady State Response)

In order to study the control of the system, the control constants must be specified for each case of operation. A detailed analysis of the system can be made with the aid of controlled variables.

Defining the dynamic temperature response as the percentage of response gained at time  $t=0$  to the ultimate response at  $t=\infty$  [30], so

$$T_i'(t) = \frac{T_{i,t} - T_{i,\infty}}{\Delta T_{i,\max}} \quad (3.1)$$

where

$$\Delta T_{i,\max} = T_{i,\infty} - T_{i,0} \quad (3.2)$$

The unsteady state dynamic temperature response can be defined in an alternative way as [31]

$$T_i^R(t) = 100 \left( 1 - \exp\left(-\frac{t}{\tau}\right) \right) \quad (3.3)$$

where  $\tau$  is the time constant. Equation 3.3 is a well known first order response equation for a step input change. When there is a delay in the system, equation 3.3 becomes

$$T_i^R(t) = 100 \left( 1 - \exp\left(-\frac{t - \theta}{\tau}\right) \right) \quad (3.4)$$

where  $\theta$  is the dead time or delay time.



## Chapter Four

### Calculations and Interpretations

#### 4.1 Theoretical Calculations of the Heat Exchanger Parameters

##### 4.1.1 NTU method of analysis

The effectiveness of the heat exchanger can be easily determined using experimental data.

For cross flow with both fluids unmixed, the following equation can be used

$$\varepsilon = 1 - \exp \left[ \frac{\left( \exp \left[ -CN^{0.78} \right] - 1 \right)}{CN^{-0.22}} \right] \quad (4.1)[32]$$

where

$$N = \frac{UA}{C_{\min}} \quad (4.2)$$

$$C = \frac{C_{\min}}{C_{\max}} = \frac{(m^{\circ}c_p)_{\min}}{(m^{\circ}c_p)_{\max}} \quad (4.3)$$

The effectiveness is defined as

$$\varepsilon = \frac{\Delta T_{\min}}{\Delta T_{\max}} \quad (4.4)$$

The specific heat capacity of water at 60°C is 4.179 KJ / Kg.°C

The density equal 983.3Kg/m<sup>3</sup>

The volumetric flow rate of water is 1.4 x10<sup>-4</sup> m<sup>3</sup>/s

$$m^{\circ} = Q\rho = 983.3 \times 1.4 \times 10^{-4} = 0.137 \text{Kg} / \text{s}$$

$$(m^{\circ}c_p)_h = 0.137 \times 4.179 = 0.571 \text{Kw} / ^{\circ}\text{C}$$

The specific heat capacity of air at 34°C is 1.0065 KJ / Kg.°C

The density equal 1.135 Kg/m<sup>3</sup>

The volumetric flow rate of air for the first test is 0.035 m<sup>3</sup>/s

$$\dot{m} = Q\rho = 1.135 \times 0.35 = 0.04 \text{ Kg / s}$$

$$(\dot{m} c_p)_c = 0.4 \times 1.0065 = 0.0403 \text{ Kw / } ^\circ\text{C}$$

∴ air is the minimum fluid for the first test

$$\varepsilon = \frac{T_{a,out} - T_{a,in}}{T_{w,in} - T_{a,in}} = \frac{41 - 34}{60 - 34} = 0.27$$

$$C = \frac{0.0403}{0.571} = 0.071$$

Solving for N gives

$$N = 0.32$$

$$UA = 0.32 \times 0.0403 = 0.0129 \text{ KW / } ^\circ\text{C}$$

For the second test

The volumetric flow rate of air for the second test is  $0.041 \text{ m}^3/\text{s}$

$$\dot{m} = Q\rho = 1.135 \times 0.041 = 0.047 \text{ Kg / s}$$

$$(\dot{m} c_p)_c = 0.047 \times 1.0065 = 0.0473 \text{ Kw / } ^\circ\text{C}$$

∴ air is the minimum fluid for the second test

$$\varepsilon = \frac{T_{a,out} - T_{a,in}}{T_{w,in} - T_{a,in}} = \frac{42 - 34}{60 - 34} = 0.31$$

$$C = \frac{0.0473}{0.571} = 0.0828$$

Solving for N gives

$$N = 0.38$$

$$UA = 0.38 \times 0.0473 = 0.0179 \text{ KW / } ^\circ\text{C}$$

The volumetric flow rate of air for the third test is  $0.045 \text{ m}^3/\text{s}$

$$\dot{m} = Q\rho = 1.135 \times 0.045 = 0.051 \text{ Kg / s}$$

$$(\dot{m} c_p)_c = 0.051 \times 1.0065 = 0.0514 \text{ Kw / } ^\circ\text{C}$$

∴ Air is the minimum fluid for the second test

$$\varepsilon = \frac{T_{a,out} - T_{a,in}}{T_{w,in} - T_{a,in}} = \frac{44 - 34}{60 - 34} = 0.38$$

$$C = \frac{0.0514}{0.571} = 0.09$$

Solving for N gives

$$N = 0.50$$

$$UA = 0.50 \times 0.0514 = 0.0257 \text{ KW } / ^\circ\text{C}$$

$$A_o = n\pi L(OD) = 18 \times 2 \times \pi \times 0.0045 \times 0.2 = 0.102 \text{ m}^2$$

So, a table can be constructed for the system as following.

**Table 4.1** Theoretical values of the overall heat transfer coefficient.

Run	Effectiveness	NTU	U (W / m <sup>2</sup> .°C )
1	0.27	0.32	126
2	0.31	0.38	175
3	0.38	0.50	252

#### 4.1.2 Water side heat transfer coefficient

For the water side the temperature in was 60°C and at this temperature the following data was obtain:

$$C_p = 4.179 \times 10^3 \text{ j/kg.}^\circ\text{C}$$

$$\rho = 983.3 \text{ kg/m}^3$$

$$\mu = 4.71 \times 10^{-4} \text{ kg/m.s}$$

$$k = 0.654 \text{ W/m.}^\circ\text{C}$$

$$\text{Pr} = 3.01$$

The volumetric flow rate is constant and equals 0.000139 m<sup>3</sup>/sec

The heat exchanger inside configuration is as following:

The inside diameter of the pipes is 0.004 m

The number of pipes is 18

Each pipe has a length of 0.20 m

So, the inner area can be calculated from as following:

Inside cross-sectional area =  $A_{ic} = \pi ID^2/4$

$$A_{ic} = 1.26 \times 10^{-5} \text{ m}^2$$

The water velocity can be calculated since the volumetric flow rate and the inside cross sectional area are available

$$u_{wm} = Q_w / nA_{ic}$$

$$u_{wm} = 0.613 \text{ m/s}$$

Then, the Reynold number can be calculated easily

$$Re = \frac{\rho u_{wm} ID}{\mu} = \frac{983.3 \times 0.613 \times 0.004}{4.71 \times 10^{-4}} = 5118$$

After the calculation of Reynold number, the L/ID is calculated to find the proper equation for the calculation of Nusselt number and then the inside heat transfer coefficient

$$Nu_d = 0.023 Re_d^{0.8} Pr^n$$

where

n=0.4 for heating

n=0.3 for cooling

0.6 < Pr < 100

2500 < Re < 1.25 × 10<sup>5</sup>

So,

$$Nu_d = \frac{h_i \times ID}{k} = \frac{h_i \times 0.004}{0.654} = 0.023 (5118)^{0.8} (3.01)^{0.3}$$

$$h_i = 4854 \text{ W/m}^2 \cdot \text{s}$$

The heat transfer coefficient for the air side can not easily obtained because of the lack of information connecting velocity variation with heat transfer coefficient on the air side for this particular type of heat exchanger. So, a

backward method is done by using the NTU method to obtain the overall heat transfer coefficient (U) and then finding the heat transfer coefficient on the air side.

#### 4.1.3 Air side heat transfer coefficient

To evaluate the overall heat transfer coefficient, the total thermal resistance method is used where

$$\frac{1}{UA_a} = \left( \frac{1}{h_a A_a} + \frac{1}{h_w A_w} \right) \quad (4.5)$$

Equation 4.4 can be rearranged into an alternative form

$$h_a = \frac{1}{A_a} \left( \frac{1}{UA_a} - \frac{1}{h_w A_w} \right)^{-1} \quad (4.6)$$

The values of air side heat transfer coefficient is shown in the following table

**Table 4.2** Air side heat transfer coefficient.

Run	$Q_a$ (m <sup>3</sup> /s)	U (W / m <sup>2</sup> .°C)	$h_a$ (W / m <sup>2</sup> .°C)
1	0.035	126	130
2	0.041	175	182
3	0.045	252	268

From table 4.2 it is evident that the heat transfer coefficient is increased by increasing the flow rate of hot air. It is also noticeable that the increment is too low compared with the value of the water side heat transfer coefficient. Now, relating drawing the flow rate versus air side heat transfer coefficient gives the following figure.

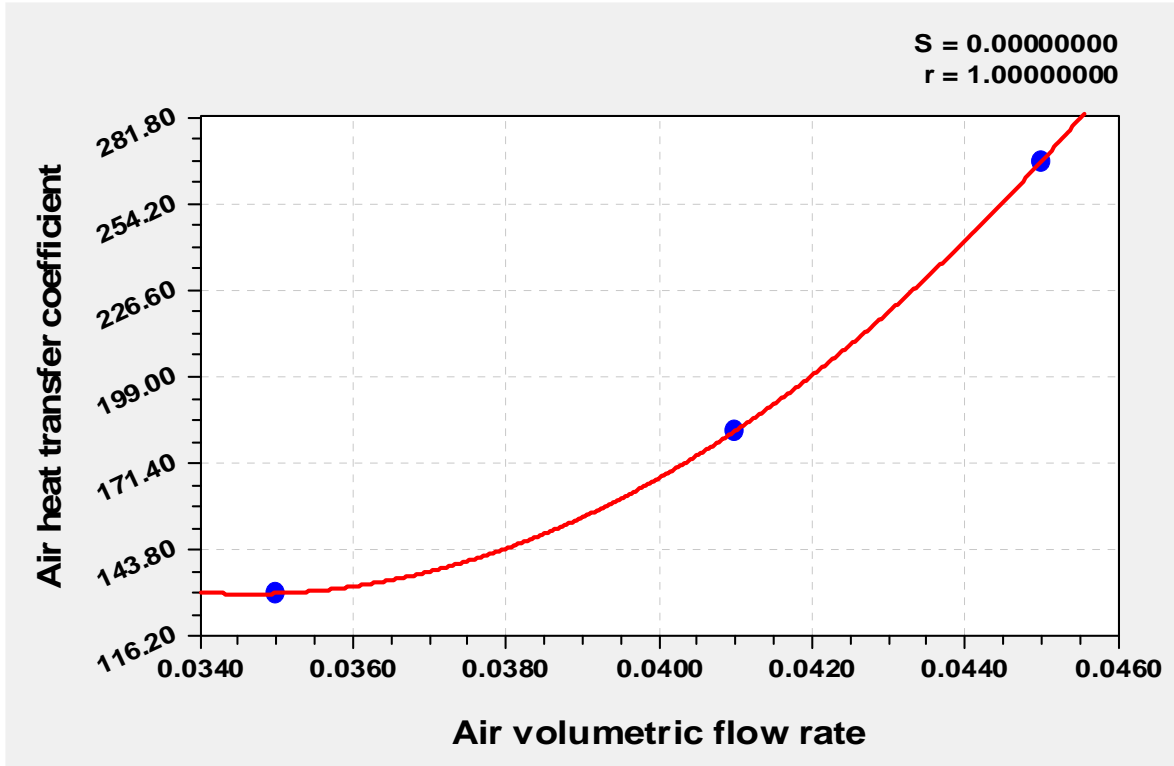


**Fig. 4.1** Air heat transfer coefficient versus air volumetric flow rate.

Quadratic Fit of the data yields

$$h_a = 1668.25 - 88.9 \times 10^3 Q_a + 12.8 \times 10^5 Q_a^2 \quad (4.7)$$

#### 4.1.4 Theoretical Simulation Using NTU Method

Using different flow rates of both air and water to analyze the system independently for a larger range than that of experimental work will give a better understanding of the factors that have the biggest influence on system performance.

- i) Effect of Flow Rate Variation on the Overall Heat Transfer Coefficient

Air heat transfer coefficient can be obtained directly from equation 4.7 while that for water need the procedure of section 4.1.2 to be repeated.

The following curve shows the effect of changing flow rate of water and air on the overall heat transfer coefficient.

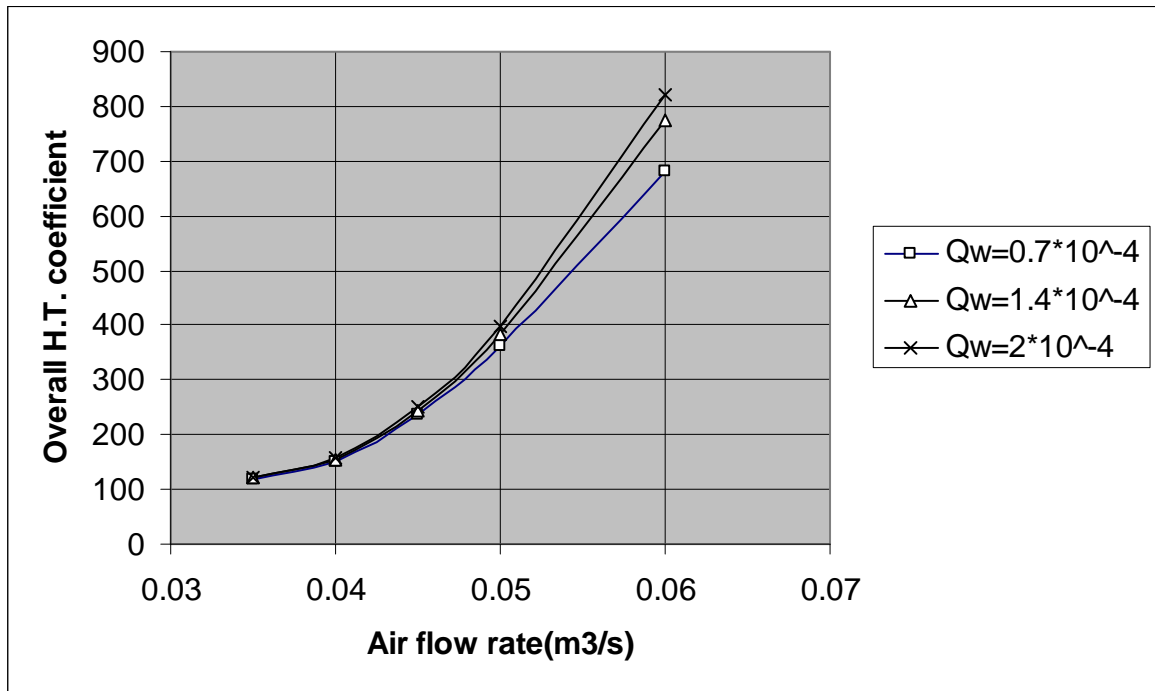


**Fig. 4.2** Overall heat transfer coefficient change with volumetric flow rate of air.

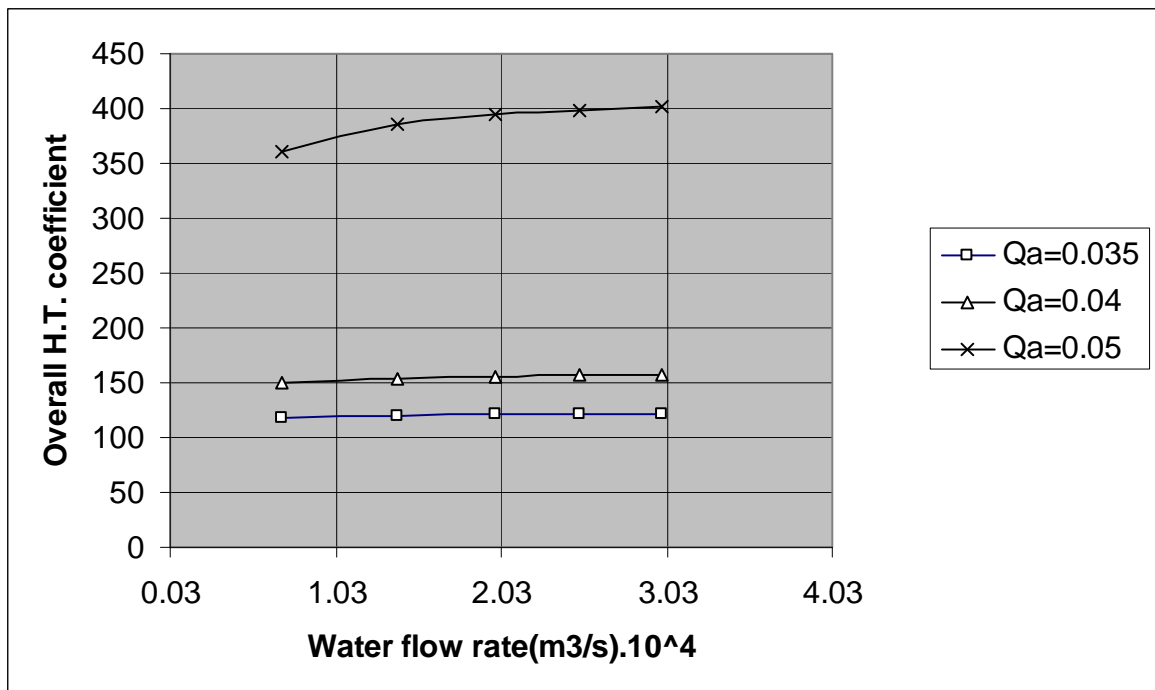


**Fig. 4.3** Overall heat transfer coefficient change with volumetric flow rate of water.

ii) Effect of Flow Rate on Effectiveness

The effect of increasing water or air flow rate on effectiveness has been predicted from the former equations. The following figure shows the effectiveness variation with flow rate change.

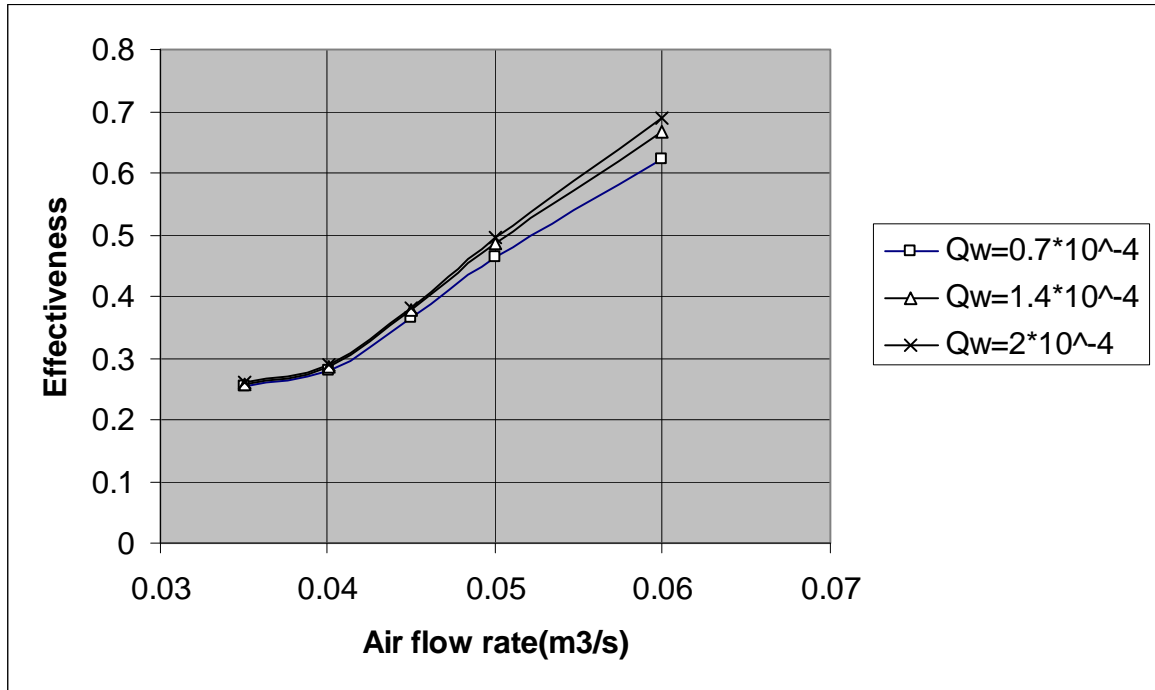


**Fig. 4.4** Effectiveness versus air flow rate at different water flow rates.



## 4.2 Control of Heat Exchanger

Studying the control of the system for the three tests in order to find the time constant  $\tau$  and the dead time  $\theta$  for each case.

### 4.2.1 Control Constants of the First Test

From table 3.2 the maximum temperature difference for air side is  $7^\circ$  and for water side is  $5^\circ$ . Assuming a step input change from the initial state will give full analysis of the system.

Defining the response variables in the following way for both air and water temperatures responses (T.R.) as  $T'_a(t)$  and  $T'_w(t)$  respectively

a) Air Side

$$T'_a(t) = \frac{T_{a,t} - T_\infty}{\Delta T_{a,\max}} 100\% \quad (4.8)$$

where

$$\Delta T_{a,\max} = T_{a,\infty} - T_{a,0} \quad (4.9)$$

The following table can be constructed for the air temperature response.

**Table 4.3** Air temperature response with time for the first test.

Time (min)	$T_{a,t}$	$T'_a(t)$
0	34	0
0.5	36	28.34687
1	39	68.85968
1.5	39.7	86.46647
2	40	94.11835
2.5	40.2	97.44385
3	40.5	98.8891
3.5	40.8	99.51721
4	40.8	99.79018
4.5	41	99.90881
5	41	99.96037
7	41	99.99859

Air temperature response of the first test is drawn as shown below.

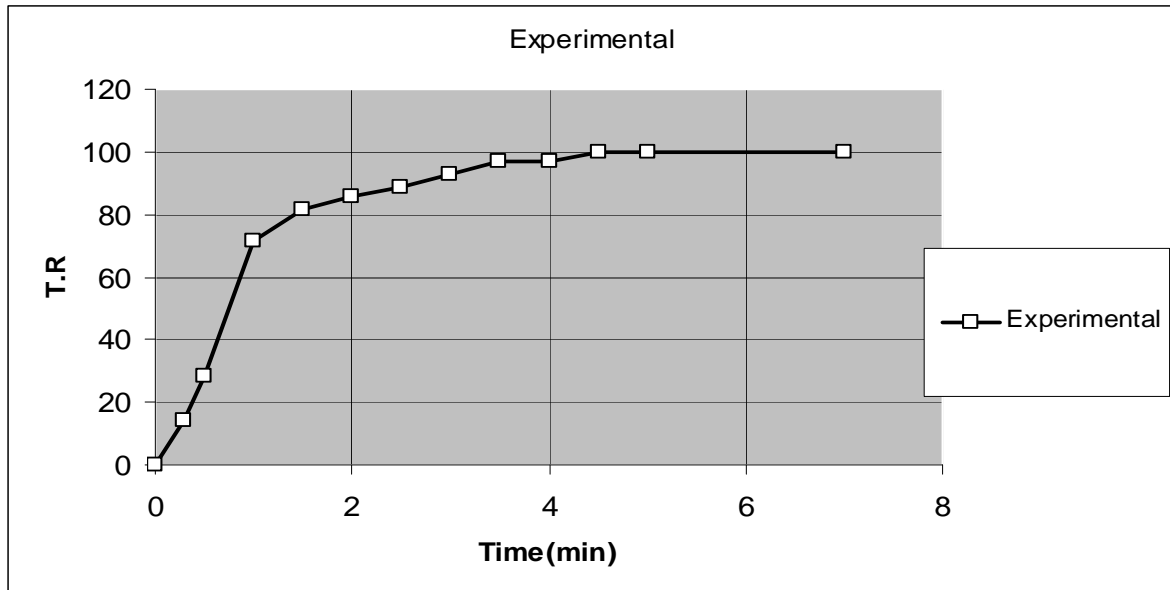


**Fig.4.5** Air temperature response for the first test.

Reading the  $t_1$  and  $t_2$  for 28.3 and 63.2% air temperature responses.

$$t_1=0.5 \text{ min} \quad : \quad t_2=0.9 \text{ min}$$

so, the time constant and the dead time can be calculated as

$$\tau = 1.5(t_2 - t_1) = 1.5(0.9 - 0.5) = 0.6 \text{ min}$$

and the dead time

$$\theta = t_2 - \tau = 0.9 - 0.6 = 0.3 \text{ min}$$

The air dynamic temperature response  $T_a^R(t)$  can be calculated as following

$$T_a^R(t) = 100 \left( 1 - \exp \left( -\frac{t - \theta}{\tau} \right) \right)$$

Drawing the air dynamic temperature response will give the following figure

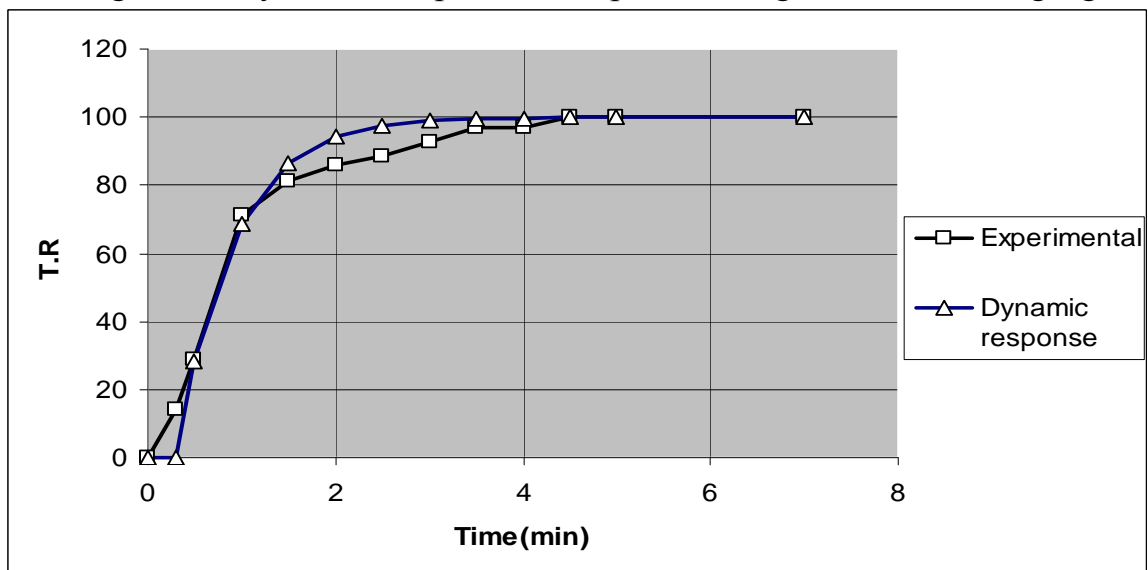


**Fig.4.6** Experimental and dynamic T.R. of air for the first test.

b) Water Side

$$T_w'(t) = \frac{T_{w,t} - T_{w,in}}{\Delta T_{w,max}}$$

where

$$\Delta T_{w,max} = T_{w,\infty} - T_{w,0}$$

The following table can be constructed for the water temperature response.

**Table 4.4** Water temperature response with time for the first test.

Time (min)	$T_{w,t}$	$T_w'(t)$
0	60	0
0.5	59	10.51607
1	58.5	32.21904
1.5	57.8	48.65829
2	57	61.11044
2.5	56.5	70.54252
3	56	77.68698
3.5	55.8	83.09867
4	55.4	87.19783
4.5	55	90.3028
5	55	92.65471
7	55	97.58198

water temperature response of the first test is drawn as shown below.

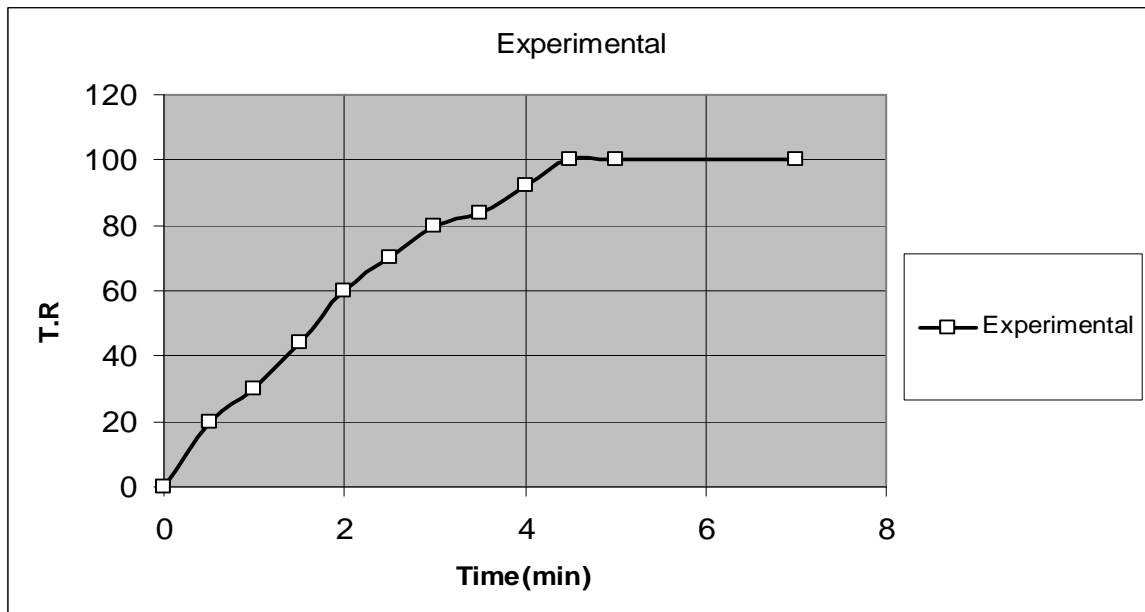


**Fig.4.7** Water temperature response for the first test.

Reading the  $t_1$  and  $t_2$  for 28.3 and 63.2% air temperature responses.

$$t_1=0.9 \text{ min} \quad : \quad t_2=2.1 \text{ min}$$

so, the time constant and the dead time can be calculated as

$$\tau = 1.5(t_2 - t_1) = 1.5(2.1 - 0.9) = 1.8 \text{ min}$$

and the dead time

$$\theta = t_2 - \tau = 2.1 - 1.8 = 0.3 \text{ min}$$

The water dynamic temperature response  $T_w^R(t)$  can be calculated as following

$$T_w^R(t) = 100 \left( 1 - \exp\left(-\frac{t - \theta}{\tau}\right) \right)$$

Drawing the water dynamic temperature response will give the following figure

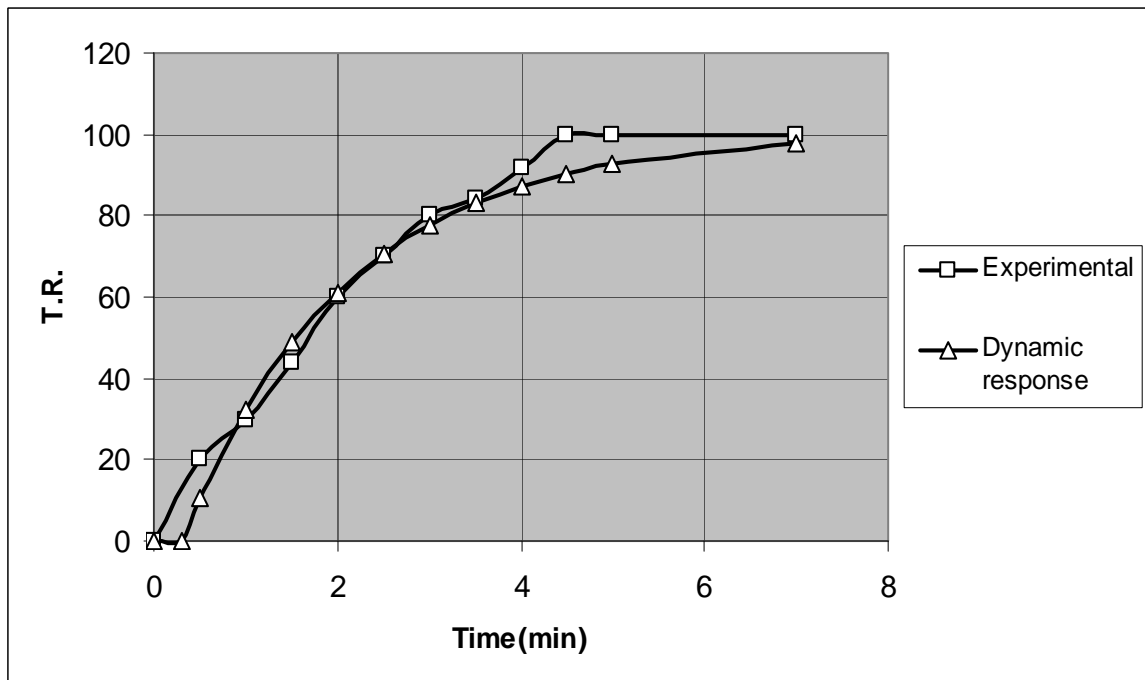


**Fig.4.8** Experimental and dynamic temperature response of water for the first test.

#### 4.2.2 Control Constants of the Second Test

From table 3.4 the maximum temperature difference for air side is  $8^\circ$  and for water side is  $6.5^\circ$ .

a) Air Side

The following table can be constructed for the air temperature response.

**Table 4.5** Air temperature response with time for the second test.

Time (min)	$T_{a,t}$	$T_a'(t)$
0	34	0
0.5	37	40.41287
1	40	70.68147
1.5	40.5	85.57446
2	40.8	92.90223
2.5	41.2	96.5077
3	41.6	98.28169
3.5	41.8	99.15454
4	42	99.58401
4.5	42	99.79532
5	42	99.89929

Air temperature response of the second test is drawn as shown below.

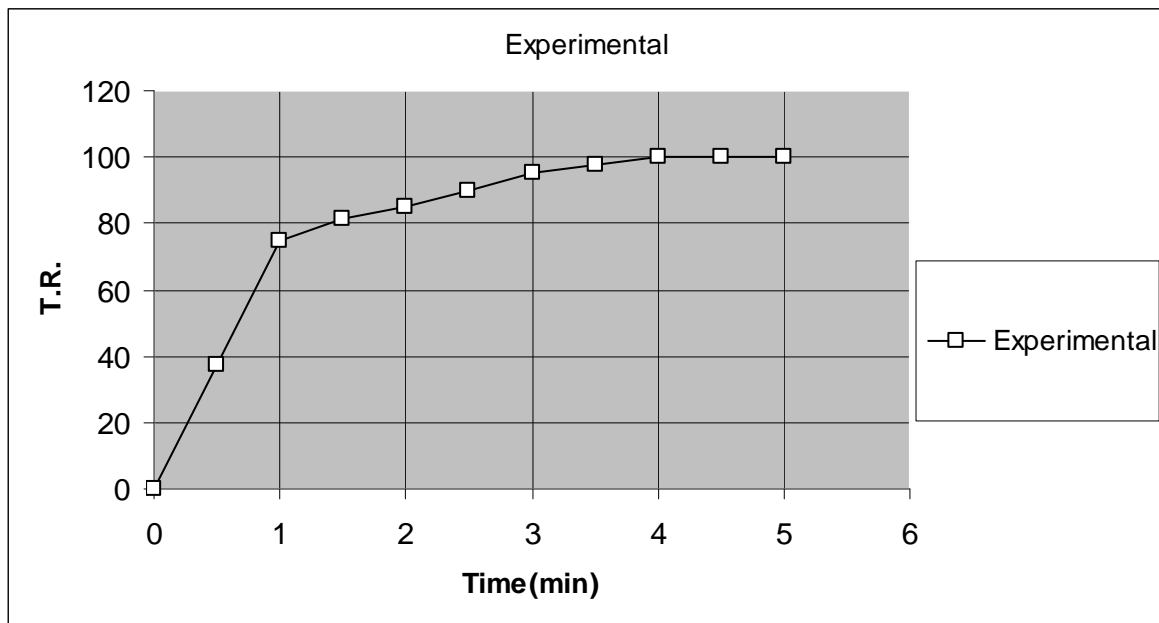


**Fig.4.9** Air temperature response for the second test.

Reading the  $t_1$  and  $t_2$  for 28.3 and 63.2% air temperature responses.

$$t_1=0.37 \text{ min} : t_2=0.84 \text{ min}$$

so, the time constant and the dead time can be calculated as

$$\tau = 1.5(t_2 - t_1) = 1.5(0.84 - 0.37) = 0.705 \text{ min}$$

and the dead time

$$\theta = t_2 - \tau = 0.84 - 0.705 = 0.135 \text{ min}$$

The air dynamic temperature response  $T_a^R(t)$  can be calculated as following

$$T_a^R(t) = 100 \left( 1 - \exp\left(-\frac{t - \theta}{\tau}\right) \right)$$

Drawing the air dynamic temperature response will give the following figure

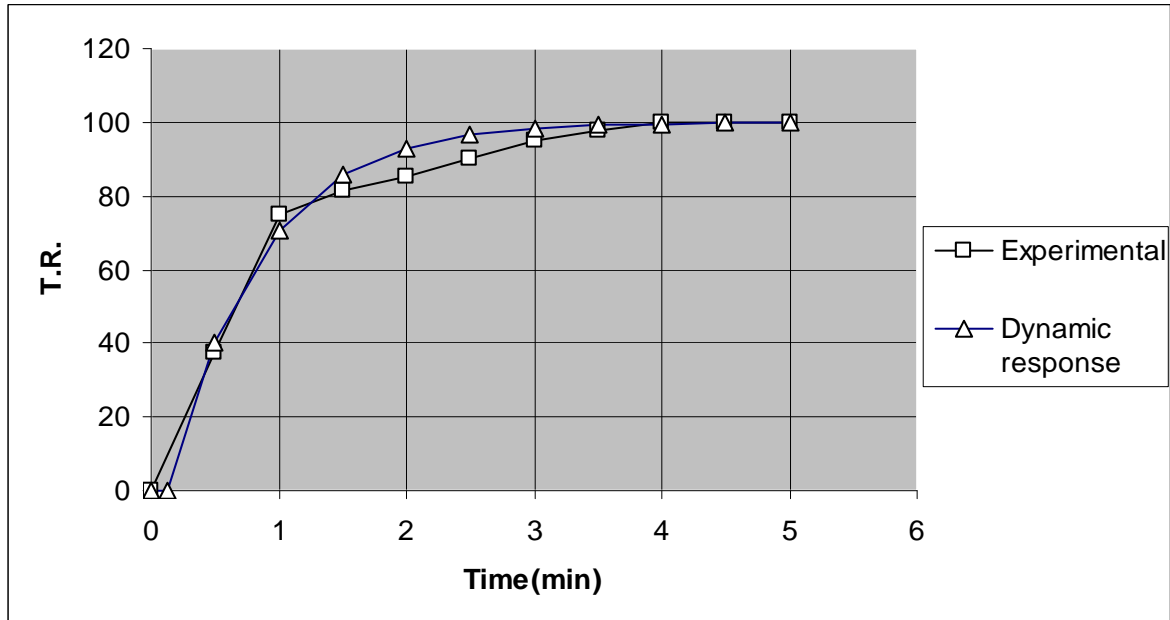


**Fig.4.10** Experimental and dynamic temperature response of air for the second test.

b) Water Side

The following table can be constructed for the water temperature response.

**Table 4.6** Water temperature response with time for the second test.

Time (min)	$T_{w,t}$	$T_w'(t)$
0	60	0
0.5	58.5	20.39316
1	57	43.9512
1.5	56	60.53771
2	55	72.21577
2.5	54.5	80.43795
3	54	86.22695
3.5	53.8	90.3028
4	53.5	93.17249
4.5	53.5	95.19296
5	53.5	96.6155
7	53.5	99.16832

Water temperature response of the second test is drawn as shown below.

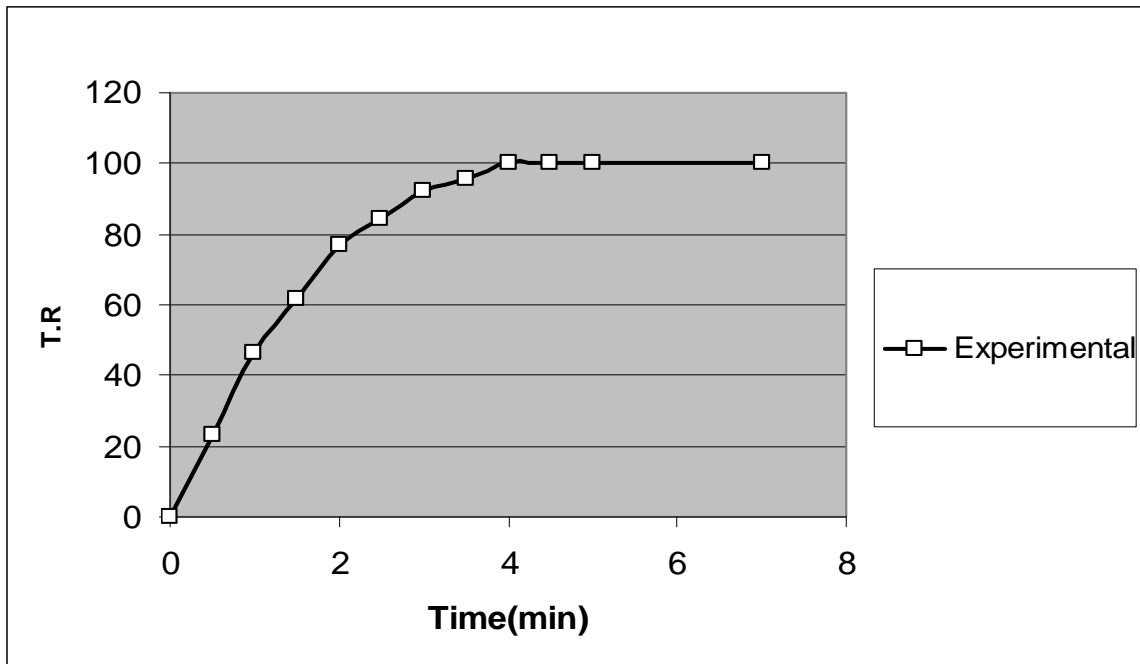


**Fig.4.11** Water temperature response for the second test.

Reading the  $t_1$  and  $t_2$  for 28.3 and 63.2% air temperature responses.

$$t_1=0.65 \text{ min} : t_2=1.6 \text{ min}$$

so, the time constant and the dead time can be calculated as

$$\tau = 1.5(t_2 - t_1) = 1.5(1.6 - 0.65) = 1.425 \text{ min}$$

and the dead time

$$\theta = t_2 - \tau = 1.6 - 1.425 = 0.175 \text{ min}$$

The water dynamic temperature response  $T_w^R(t)$  can be calculated as following

$$T_w^R(t) = 100 \left( 1 - \exp \left( -\frac{t - \theta}{\tau} \right) \right)$$

Drawing the water dynamic temperature response will give the following figure

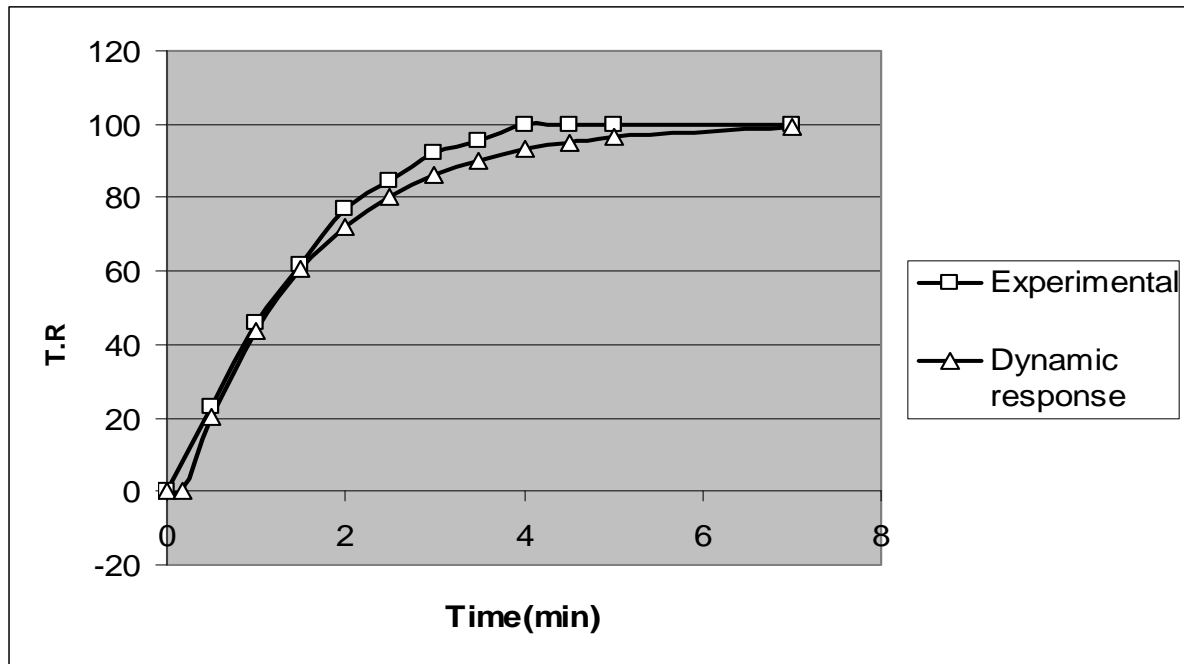


**Fig.4.12** Experimental and dynamic temperature response of water for the second test.

### 4.2.3 Control Constants of the Third Test

From table 3.6 the maximum temperature difference for air side is  $10^{\circ}$  and for water side is  $9^{\circ}$

a) Air Side

The following table can be constructed for the air temperature response.

**Table 4.7** Air temperature response with time for the third test.

Time (min)	$T_{a,t}$	$T_a'(t)$
0	34	0
0.5	38	37.63851
1	41	64.21988
1.5	41.5	79.47103
2	42	88.22144
2.5	42.3	93.24201
3	43	96.12258
3.5	43.5	97.77532
4	44	98.72358
4.5	44	99.26765
5	44	99.57981

Air temperature response of the third test is drawn as shown below.



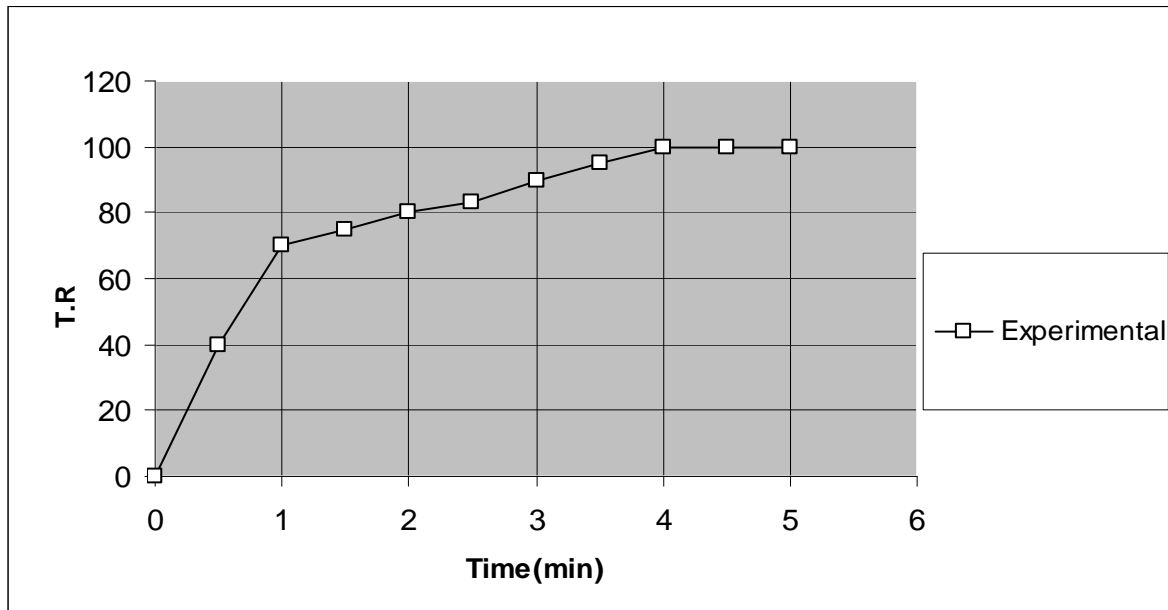


**Fig.4.13** Air temperature response for the third test.

Reading the  $t_1$  and  $t_2$  for 28.3 and 63.2% air temperature responses.

$$t_1=0.375\text{min} : t_2=0.975\text{min}$$

so, the time constant and the dead time can be calculated as

$$\tau = 1.5(t_2 - t_1) = 1.5(0.975 - 0.375) = 0.9 \text{ min}$$

and the dead time

$$\theta = t_2 - \tau = 0.975 - 0.9 = 0.075 \text{ min}$$

The air dynamic temperature response  $T_a^R(t)$  can be calculated as following

$$T_a^R(t) = 100 \left( 1 - \exp \left( -\frac{t - \theta}{\tau} \right) \right)$$

Drawing the air dynamic temperature response will give the following figure

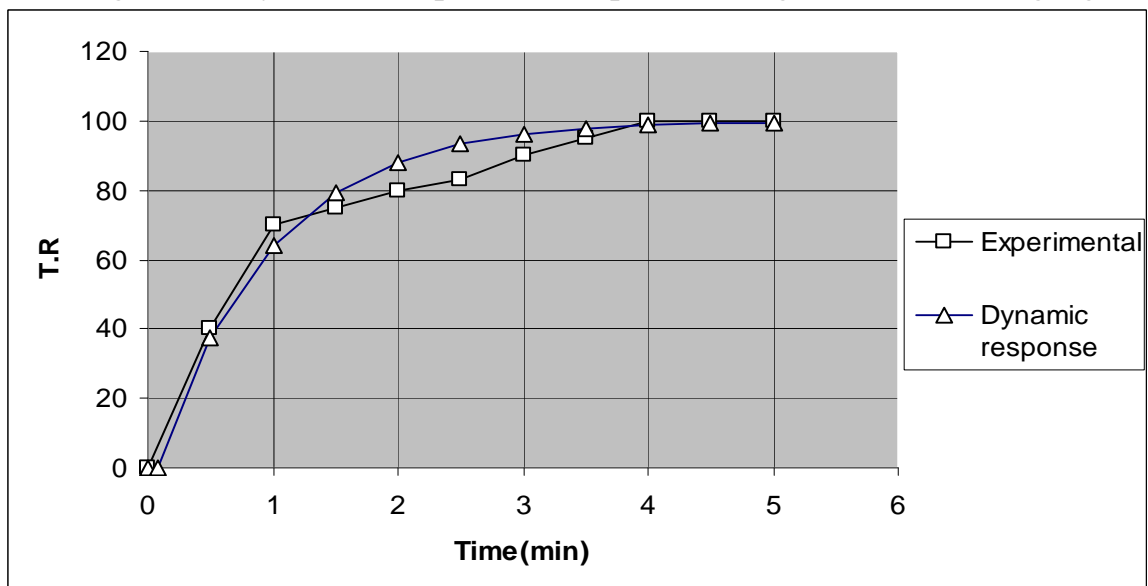


**Fig. 4.14** Experimental and dynamic T.R. of air for the third test.

b) Water Side

The following table can be constructed for the water temperature response.

**Table 4.8** Water temperature response with time for the third test.

Time (min)	$T_{w,t}$	$T_w'(t)$
0	60	0
0.5	58.5	15.83692
1	57	33.12191
1.5	56	46.85701
2	55	57.77125
2.5	54	66.44398
3	53	73.33555
3.5	52	78.81177
4	51.5	83.1633
4.5	51	86.62114
5	51	89.36882
7	51	95.76133

water temperature response of the third test is drawn as shown below.

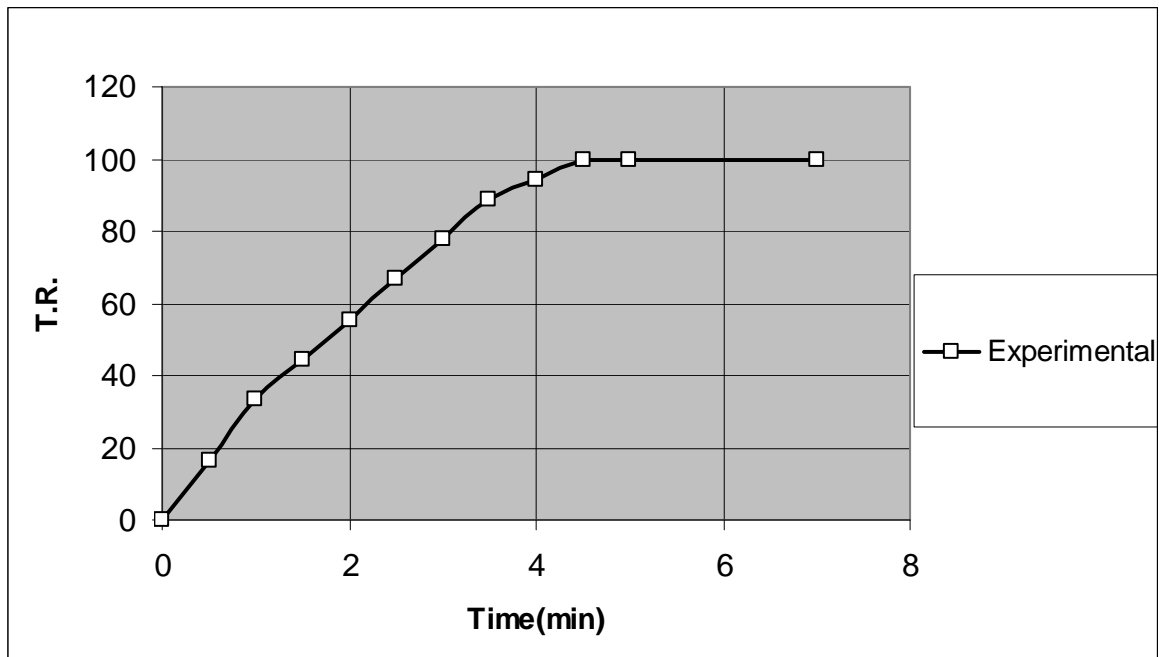


**Fig. 4.15** Water temperature response for the third test.

Reading the  $t_1$  and  $t_2$  for 28.3 and 63.2% air temperature responses.

$$t_1=0.9 \text{ min} \quad : \quad t_2=2.1 \text{ min}$$

so, the time constant and the dead time can be calculated as

$$\tau = 1.5(t_2 - t_1) = 1.5(2.3 - 0.85) = 2.175 \text{ min}$$

and the dead time

$$\theta = t_2 - \tau = 2.3 - 2.175 = 0.125 \text{ min}$$

The water dynamic temperature response  $T_w^R(t)$  can be calculated as following

$$T_w^R(t) = 100 \left( 1 - \exp\left(-\frac{t - \theta}{\tau}\right) \right)$$

Drawing the water dynamic temperature response will give the following figure

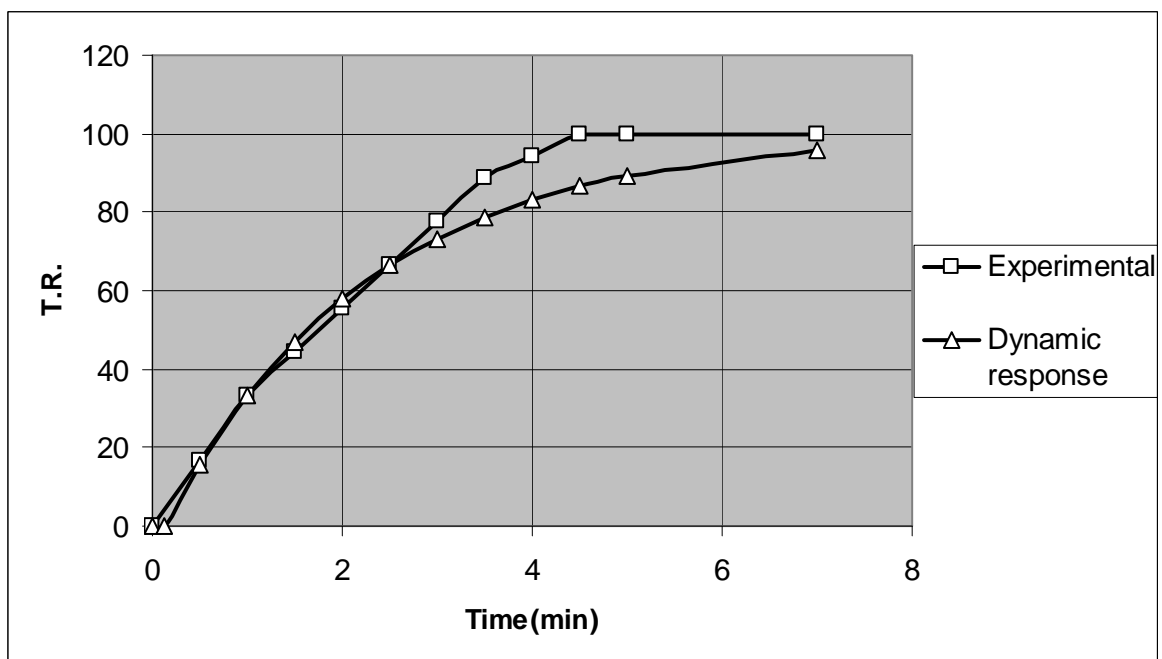


**Fig.4.16** Experimental and dynamic temperature response of water for the third test.

## Chapter Five

### Discussions

#### 5.1 Discussion of NTU Method

From the results of section 4.1 it is evident that the heat transfer is affected by the flow rate of water and air and hence larger flow rate means higher heat transfer rate. However, because of the relatively low values of heat transfer coefficient on the air side compared to the heat transfer coefficient value on the water, the heat transfer coefficient on the air side has the key role in the overall heat transfer across the heat exchanger. This can be explained by the series resistance law which states that the total resistance is the sum of the individual resistance components.

$$R = R_1 + R_2 + R_3 + \dots \quad (5.1)$$

where  $R_1, R_2, \dots etc$  are the individual resistances. In an alternative form, equation 5.1 can be written as

$$R = R_w + R_a = \frac{1}{UA_a} = \frac{1}{h_a A_a} + \frac{1}{h_w A_w} \quad (5.2)$$

where  $R_a$  and  $R_w$  are the resistances of air and water sides respectively. From equation 5.2, it is clear that the total resistance is higher than the individual resistances. Hence the resistance is the reciprocal of heat transfer coefficient. This leads to the conclusion that the overall heat transfer coefficient will be lower from both of the resistances, and from table 4.1 it will be closer to the lower value. So, increasing the flow rate of air will give a better performance than that of the water because the value of the heat transfer coefficient is already high and will

have a negligible effect on the total heat transfer. This concept is obvious from Fig. 4.2 and 4.3

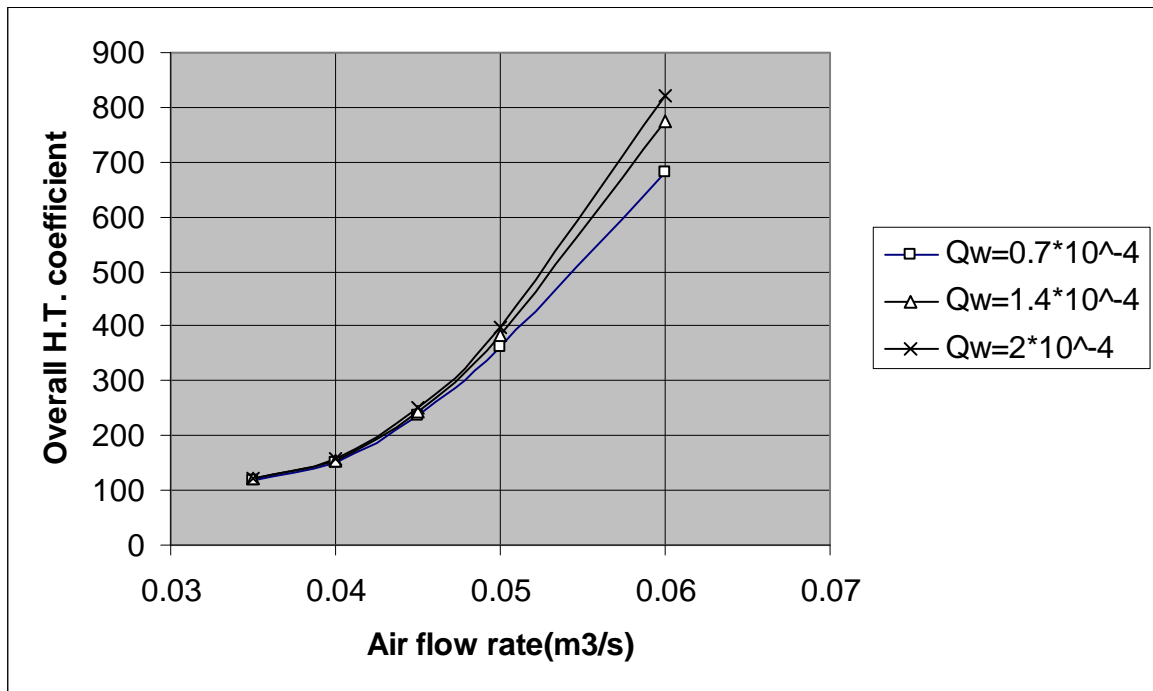


Fig. 4.2 Overall H.T. coefficient change with volumetric flow rate of air.

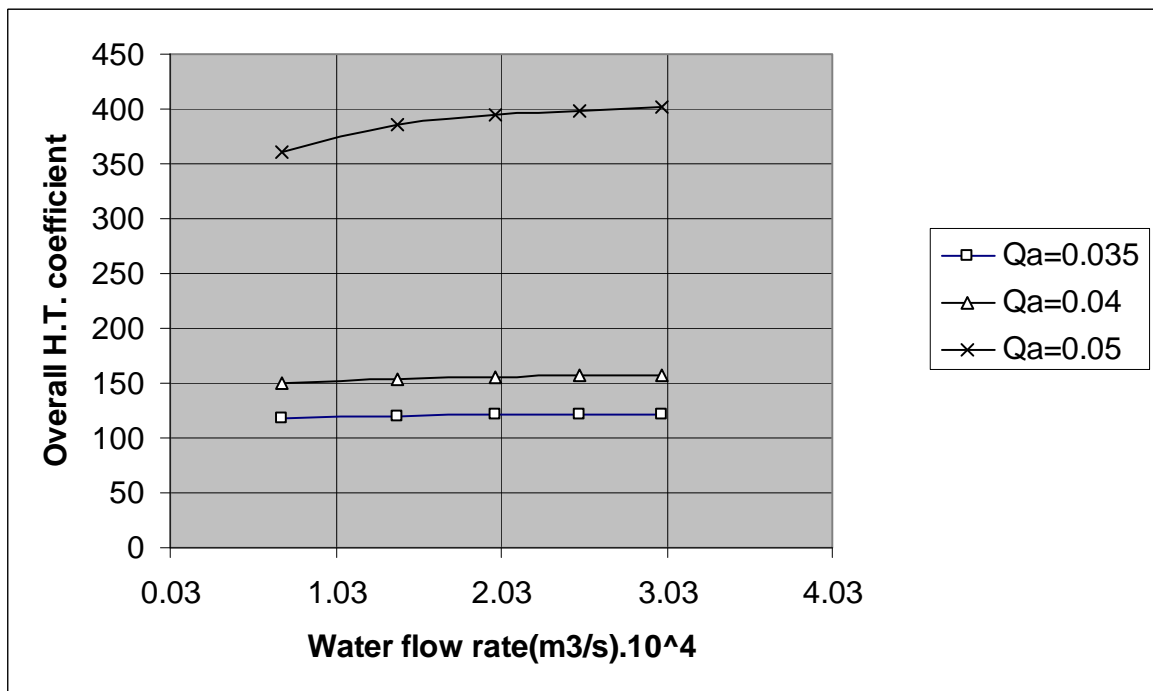
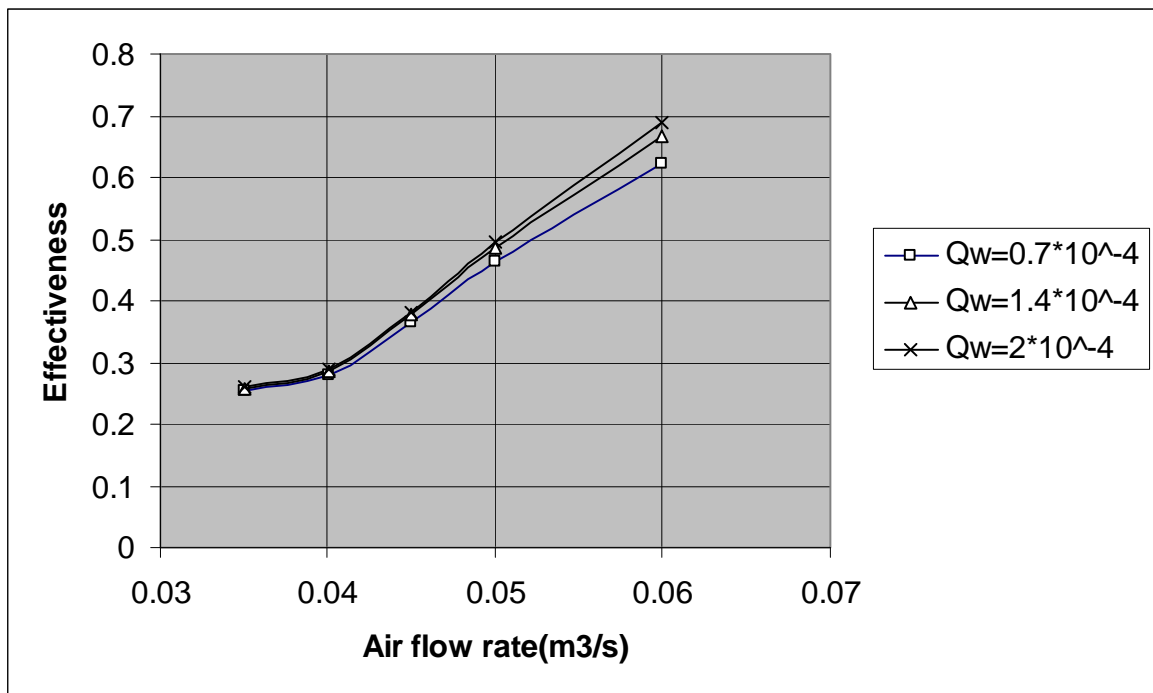


Fig. 4.3 Overall H.T. coefficient change with volumetric flow rate of water.

The effectiveness of this type of heat exchanger is relatively low and can only be increased by high air flow rate because the outlet temperature of the hot stream will still be higher than that of the cold stream; while it is possible in some cases of heat exchangers that the outlet temperature of the hot stream might possibly be lower than that of the cold stream. Fig. 4.4 shows that the effectiveness as well is not highly affected by the flow rate of water while it is sensitive to any minor change in air flow rate.



**Fig. 4.4** Effectiveness versus air flow rate at different water flow rates.

## 5.2 Discussion of the Control of Heat Exchanger

In all thermal systems, it is logical to have some delay in the system response because of the thermal inertia of the system and the thermometer. Studying the time constant which is an indication of how

fast the system will reach the steady state, and the time consumed by the system to show response. The time constant of air side has revealed an increasing pattern, because the air spends much less time in the heat exchanger when the velocity increases. As shown in the table below

**Table 5.1** Time constant and dead time for air side temperature response.

Test number	$\tau$ (min)	$\theta$ (min)
1	0.6	0.3
2	0.705	0.135
3	0.9	0.075

The dead time decreases enormously as the velocity of flow increases, since higher velocity means lower time spent in the heat exchanger which is a quite logical concept. This is also applicable in the case of time constant and dead time for the dynamic temperature response for the water side as shown in section 4.2.

Finally it is vital to mention that the error sources for the heat transfer result come from the measurements of air-side temperatures and air flow rate. Because of the low conductivity and heat transfer coefficient of air which causes a delay in the response time, it is quite usually that most of the error comes from the reading of air temperature.

## **Chapter Six**

### **Conclusions and Recommendations**

#### **6.1 Conclusions**

From the former work it is found that compact heat exchangers are useful device in industry. A number of conclusions have been reached:

- 1) Changing water flow rate has a minor effect on heat transfer rates, while air has the key role on heat transfer.
- 2) Increasing flow rate will enhance the response of the system and reduce the dead time.
- 3) Effectiveness has been proved that it is highly affected by air flow rate, while water flow rate has smaller effect on it.
- 4) The heat transfer in this system will be affected by the mass of the metal in the heat exchanger which causes a delay in the heat transfer because an amount of energy will be preserved in the metal.
- 5) These systems are exceptionally useful for the application of gas liquid systems in favor of high transfer rates of energy.

#### **6.2 Recommendations:**

There are several topics that have been left out of the scope in the present thesis. These are related to the analysis of heat exchangers, and the analysis and complementary applications of the techniques used in the current work in order to improve their capabilities. Thus, some recommendations for further work in these areas are provided.

- 1- Different compact heat exchangers should be chosen for heat transfer tests, at different flow rates, so that the effect of fin spacing, number of tubes rows, fin pitch and other geometrical parameters can be concerned.



- 2- Based on the experimental data of different heat exchangers, general heat transfer correlations at different flow rates for both water-side and air-side should be correlated, in which the above geometrical effects should be taken into account.
- 3- More sophisticated dynamical models should be applied to simulate the dynamical response of heat exchangers.
- 4- The results of the different heat transfer parameters will be more accurate if the system control was by using the computer. A data acquisition card is recommended to give more accurate results, since this card able to convert analog signals comes from the sensors (e.g. thermocouples, etc...) to digital signals so that the computer will deal with these signals easily

## References:

1. Dohoy J. and Dennis N. A. "Numerical Modeling of Cross Flow Compact Heat Exchanger with Louvered Fins using Thermal Resistance Concept", SAE International, 2006-01-0726,(2006) .
2. Hewitt G.F., "Heat Exchanger Design Handbook", Begell House, (1998).
3. Hewitt G.F., Shires G.L., and Bott T.R, " Process Heat Transfer", CRC Press, (1994).
4. Kenneth Bell J., "Heat Exchangers", Encyclopedia of physical Science and Technology, Chemical Engineering Volume, 251, 3rd edition, (2003).
5. Kakac S., and Liu H., "Heat Exchangers: Selection, Rating, and Thermal Design", CRC Press, (1998).
6. Diaz G., Sen M., Yang K.T., and McClain R.L., "Simulation of Heat Exchanger Performance by Artificial Neural Networks", International Journal of HVAC, 5, 3, 195, (1999).
7. Creed T., "Measurement of Finned-Tube Heat Exchanger Performance", a Master of Mechanical Engineering Thesis, Georgia Institute of Technology, December 2004.
8. Robert H., Green Donald W., and Don Green, "Perry's Chemical Engineers' Handbook", Mc-Graw Hill Professional, 7th edition, (1997).
9. Afgan N. H., and Schlunder E. U. , " Heat Exchanger : Design and Theory " , McGraw Hill ,(1974) .
10. Hesselgreaves J.E. ,"Compact Heat Exchanger ,Selection, Design ,and Operation", Elsevier Science & Technology Books, (2001) .
11. GPSA Engineering Handbook , Section 9, (1998).
12. Tochon P., Maugey C. , and Pra F.,"The Use of Compact Heat Exchangers Technologies for The High Temperature Reactors

- Recuperators Application per Proper Design", 2<sup>nd</sup> International Topical Meeting on High Temperature Reactor Technology, Beijing, China, (2004) .
13. Marriots J., "Where and How To Use Plate Heat Exchangers", Chemical Engineering, April, (1971) .
  14. Kerner J., "Sizing Plate Exchangers", Chemical Engineering, November (1993) .
  15. Hargis A., Beckman A. , and Loicano J. , "Applications of Spiral Plate Heat Exchangers", Chemical Engineering Progress , July (1967) .
  16. Noble M.A. , Kamalani J.S. , and Mc Ketta J.J. , "Heat Transfer in Spiral Coils " , Petroleum Engineer , April (1952) .
  17. Shah, R.K., and Bhatti M.S. , "Handbook of Single Phase Convective Heat Transfer " , Chapter 3 , John Wiley and Sons, New York , (1987) .
  18. Kays, W.M. , and London A. L. , "Compact Heat Exchanger", 3<sup>d</sup> Edition , Mc Graw Hill , (1984) .
  19. Holman J.P., "Heat Transfer", Mc-Graw Hill International Editions, 8th edition, (1999).
  20. Wang C.C. , "Recent Progress on The Air – Side Performance of Fin – and – Tube Heat Exchangers", International Journal of Heat Exchangers , Vol.1 , (2000) .
  21. Sheffield J.W ., Wood R.A. , and Sauer Jr. H.J. , "Experimental Investigation of Thermal Conductance of Finned Tube Contacts" , Experimental Thermal and Fluid Science , Vol.2 , Issue 1, (1989) .
  22. Idem S.A., Jung C., Gonzalez G.G., and Goldschmidt V.M., "Performance of Air Water Copper Finned Tube Heat Exchanger at Moderate Low Air Side Reynolds Numbers Including Effect of Baffles", International Journal Of Heat and Mass Transfer", 30, 8, 1733, (1987).

23. Shepherd D.G., "Performance on One Row Tube Coils With Thin Plate Fins, Low Velocity Forced Convection", Heating, Piping and Air Conditioning", 3, 137, (1956).
24. Saboya F. E. M. , Sparrow E. M. , " Local and Average Transfer Coefficients for One-Row Plate Fin and Tube Heat Exchanger Configurations , ASME, Transactions, Series C - Journal of Heat Transfer, vol. 96, p. 265-272 , (Aug. 1974) .
25. Rich D.G. , " The Effect of Fin Spacing on The Heat Transfer and Friction Performance of Multi-row, Smooth Plate Fin-and-Tube Heat Exchangers " , ASHRAE, Trans. 79,(2) , 137-145, (1973) .
26. McQuiston F. C. , "Finned Tube Heat Exchangers: State of The Art for The Air-Side . ASHRAE Trans. , 87 (1) :71-80 , (1981) .
27. Gray D.L, and Webb R.L., Heat Transfer and Friction Correlations for Plate Finned-Tube Heat Exchangers Having Plain Fins", Eighth Heat Transfer Conference, Vol. 6, 2745, (1986).
28. Yan Y. Y. , and Lin T. F. , " Evaporation Heat Transfer and Pressure Drop of Refrigerant R-134 a in a Plate Heat Exchanger " , ASME Journal of Heat Transfer , 118 (1) , 118-127 , (1999) .
29. Mirth D.R., Ramadhani S., and Hittle D.C., "Thermal Performance of Chilled Water Cooling Coils Operating at Low Water Velocities", ASHRAE Trans., 99, 1, 43, (1993).
30. Diaz G. "Simulation and Control of Heat Exchangers Using Artificial Neural Networks, Ph.D. thesis, Department of Aerospace and Mechanical Engineering. University of Notre Dame., (1999) .
31. Faller E.W., and Luttgies M.W. , "Real Time Prediction and Control of Three-Dimensional Unsteady Separated Flow Fields Using Neural Network. Journal of Aircraft (1994) .
32. Ozisik N.M., "Heat Transfer", 3rd edition, Mc-Graw Hill, (1988).

## Appendix A

### A-1 Properties of air at atmospheric pressure.

#### Properties of air at atmospheric pressure

The values of  $\mu$ ,  $k$ ,  $c_p$ , and Pr are not strongly pressure-dependent and may be used over a fairly wide range of pressures.

T, K	$\rho$ kg/m <sup>3</sup>	$c_p$ , kJ/kg · °C	$\mu \times 10^5$ , kg/m · s	$\nu \times 10^6$ , m <sup>2</sup> /s	$k$ , W/m · °C	$\alpha \times 10^4$ , m <sup>2</sup> /s	Pr
100	3.6010	1.0266	0.6924	1.923	0.009246	0.02501	0.770
150	2.3675	1.0099	1.0283	4.343	0.013735	0.05745	0.753
200	1.7684	1.0061	1.3289	7.490	0.01809	0.10165	0.739
250	1.4128	1.0053	1.5990	11.31	0.02227	0.15675	0.722
300	1.1774	1.0057	1.8462	15.69	0.02624	0.22160	0.708
350	0.9980	1.0090	2.075	20.76	0.03003	0.2983	0.697
400	0.8826	1.0140	2.286	25.90	0.03365	0.3760	0.689
450	0.7833	1.0207	2.484	31.71	0.03707	0.4222	0.683
500	0.7048	1.0295	2.671	37.90	0.04038	0.5564	0.680
550	0.6423	1.0392	2.848	44.34	0.04360	0.6532	0.680
600	0.5879	1.0551	3.018	51.34	0.04659	0.7512	0.680
650	0.5430	1.0635	3.177	58.51	0.04953	0.8578	0.682
700	0.5030	1.0752	3.332	66.25	0.05230	0.9672	0.684
750	0.4709	1.0856	3.481	73.91	0.05509	1.0774	0.686
800	0.4405	1.0978	3.625	82.29	0.05779	1.1951	0.689
850	0.4149	1.1095	3.765	90.75	0.06028	1.3097	0.692
900	0.3925	1.1212	3.899	99.3	0.06279	1.4271	0.696
950	0.3716	1.1321	4.023	108.2	0.06525	1.5510	0.699
1000	0.3524	1.1417	4.152	117.8	0.06752	1.6779	0.702
1100	0.3204	1.160	4.44	138.6	0.0732	1.969	0.704
1200	0.2947	1.179	4.69	159.1	0.0782	2.251	0.707
1300	0.2707	1.197	4.93	182.1	0.0837	2.583	0.705
1400	0.2515	1.214	5.17	205.5	0.0891	2.920	0.705
1500	0.2355	1.230	5.40	229.1	0.0946	3.262	0.705
1600	0.2211	1.248	5.63	254.5	0.100	3.609	0.705
1700	0.2082	1.267	5.85	280.5	0.105	3.977	0.705
1800	0.1970	1.287	6.07	308.1	0.111	4.379	0.704
1900	0.1858	1.309	6.29	338.5	0.117	4.811	0.704
2000	0.1762	1.338	6.50	369.0	0.124	5.260	0.702
2100	0.1682	1.372	6.72	399.6	0.131	5.715	0.700
2200	0.1602	1.419	6.93	432.6	0.139	6.120	0.707
2300	0.1538	1.482	7.14	464.0	0.149	6.540	0.710
2400	0.1458	1.574	7.35	504.0	0.161	7.020	0.718
2500	0.1394	1.688	7.57	543.5	0.175	7.441	0.730

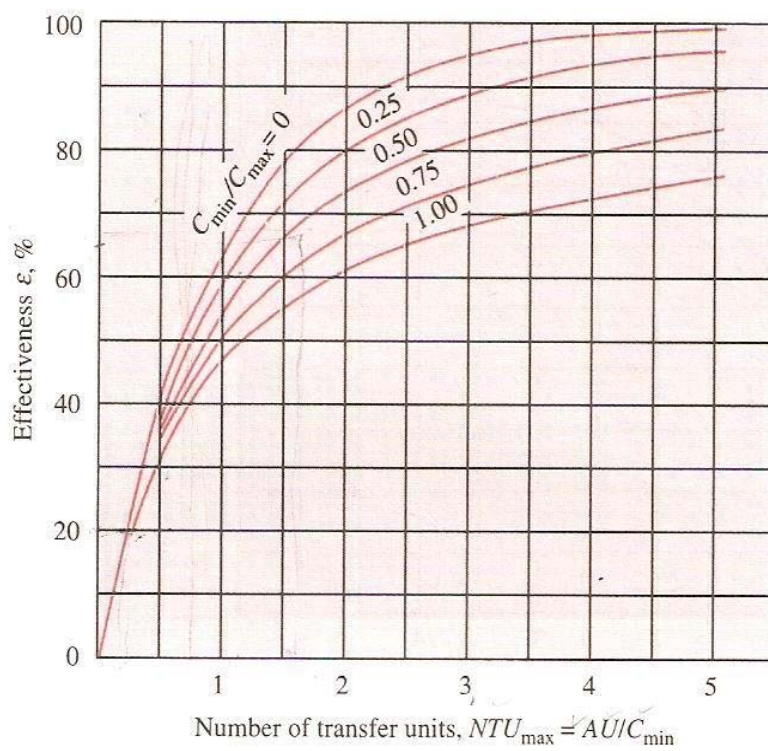
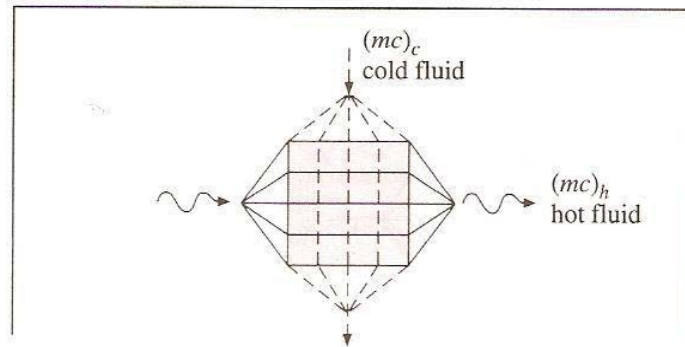
## A-2 Properties of Water

### Properties of water (saturated liquid)

Note:  $Gr_x Pr = \left( \frac{g\beta\rho^2 c_p}{\mu k} \right) x^3 \Delta T$

°F	°C	$c_p$ , kJ/kg·°C	$\rho$ , kg/m <sup>3</sup>	$\mu$ , kg/m·s	$k$ , W/m·°C	Pr	$\frac{g\beta\rho^2 c_p}{\mu k}$ , 1/m <sup>3</sup> ·°C
32	0	4.225	999.8	$1.79 \times 10^{-3}$	0.566	13.25	
40	4.44	4.208	999.8	1.55	0.575	11.35	$1.91 \times 10^9$
50	10	4.195	999.2	1.31	0.585	9.40	$6.34 \times 10^9$
60	15.56	4.186	998.6	1.12	0.595	7.88	$1.08 \times 10^{10}$
70	21.11	4.179	997.4	$9.8 \times 10^{-4}$	0.604	6.78	$1.46 \times 10^{10}$
80	26.67	4.179	995.8	8.6	0.614	5.85	$1.91 \times 10^{10}$
90	32.22	4.174	994.9	7.65	0.623	5.12	$2.48 \times 10^{10}$
100	37.78	4.174	993.0	6.82	0.630	4.53	$3.3 \times 10^{10}$
110	43.33	4.174	990.6	6.16	0.637	4.04	$4.19 \times 10^{10}$
120	48.89	4.174	988.8	5.62	0.644	3.64	$4.89 \times 10^{10}$
130	54.44	4.179	985.7	5.13	0.649	3.30	$5.66 \times 10^{10}$
140	60	4.179	983.3	4.71	0.654	3.01	$6.48 \times 10^{10}$
150	65.55	4.183	980.3	4.3	0.659	2.73	$7.62 \times 10^{10}$
160	71.11	4.186	977.3	4.01	0.665	2.53	$8.84 \times 10^{10}$
170	76.67	4.191	973.7	3.72	0.668	2.33	$9.85 \times 10^{10}$
180	82.22	4.195	970.2	3.47	0.673	2.16	$1.09 \times 10^{11}$
190	87.78	4.199	966.7	3.27	0.675	2.03	
200	93.33	4.204	963.2	3.06	0.678	1.90	
220	104.4	4.216	955.1	2.67	0.684	1.66	
240	115.6	4.229	946.7	2.44	0.685	1.51	
260	126.7	4.250	937.2	2.19	0.685	1.36	
280	137.8	4.271	928.1	1.98	0.685	1.24	
300	148.9	4.296	918.0	1.86	0.684	1.17	
350	176.7	4.371	890.4	1.57	0.677	1.02	
400	204.4	4.467	859.4	1.36	0.665	1.00	
450	232.2	4.585	825.7	1.20	0.646	0.85	
500	260	4.731	785.2	1.07	0.616	0.83	
550	287.7	5.024	735.5	$9.51 \times 10^{-5}$			
600	315.6	5.703	678.7	8.68			

### A-3 Effectiveness of cross-flow heat exchanger (Both fluids unmixed)



## الخلاصة

تستعمل المبادلات الحرارية المضغوطة بشكل واسع في العديد من تطبيقات أنظمة الموائع الحرارية وبضمنها أنظمة الإدارة الحرارية الآلية. إن المشعات الحرارية في أنظمة تبريد المحركات والمبخرات والمكثفات لأنظمة تكييف الهواء، والتبريد بمنظومات الزيوت والمبردات البينية هي أمثلة يمكن إيجادها في الحياة العملية. إن المبادلات الحرارية المضغوطة تستعمل في نقل كميات قليلة من الحرارة في أنظمة انتقال الحرارة في الطورين الغازي والسائل بسبب أملاكها مساحة تبادل حراري عالية نسبة إلى حجمها.

في هذا العمل تم استخدام مبادل حراري مضغوط أبعاده 5x19x20 سم لتبريد ماء ساخن بدرجة 60 درجة سيليزية في داخل الأنابيب باستخدام هواء بدرجة حرارة الغرفة يمر خارج الأنابيب. تم تثبيت مروحة مثبتة بحاضنة صغيرة مقارنة للمبادل الحراري. تتم السيطرة على سرعة المروحة باستخدام مفتاح فولتية وتغيير سرعة الهواء بالسيطرة على سرعة المروحة مما يؤدي إلى تغيير معدل جريان الهواء. تم استخدام ثلاثة سرعات مختلفة للهواء مع تثبيت سرعة جريان الماء. واستعملت المحارير لتسجيل التغير في درجات الحرارة للتيارات الخارجة.

لقد وجد أن العامل الرئيسي المؤثر على انتقال الحرارة هو معامل الانتقال الحراري لجانب الهواء والذي يزداد بزيادة معدل جريان الهواء بينما يكون لمعدل جريان الماء تأثير أقل على عملية انتقال الحرارة. الفعالية أيضا تسلك نفس السلوك وتزداد أيضا بزيادة معدل جريان الهواء.

إن دراسة الإستجابة الديناميكية للنظام يظهر أن ثابت الزمن لمثل هذا النظام يمكن أن يقل بزيادة معدل جريان الهواء، وهذا يعني إستجابة ديناميكية حرارية أسرع. إن وقت عدم الاستجابة يتناقص تدريجيا بزيادة معدل جريان الهواء.



## شكر وتقدير

أود أن أتقدم بالشكر الجزيل إلى مشرفي الدكتور نصير الحبوبي لجهوده الكبيرة وتوجيهاته التي ساهمت في إكمال هذا العمل . كما أتقدم بالشكر والتقدير إلى رئيس قسم الهندسة الكيماوية الأستاذ الدكتور قاسم جبار سليمان والى كادر قسم الهندسة الكيماوية من تدريسيين وإداريين لما أبدوه من مساعدة في إكمال متطلبات هذا العمل .

# دراسة خصائص إنتقال الحرارة لمبادل حراري مضغوط أثناء بدء التشغيل

رسالة

مقدمة الى كلية الهندسة في جامعة النهريين  
وهي جزء من متطلبات نيل درجة ماجستير علوم  
في الهندسة الكيماوية

من قبل

نبراس حساني عليوي العبيدي  
بكلوريوس علوم في الهندسة الكيماوية ٢٠٠٤

١٤٢٩

٢٠٠٨

محرم

كانون الثاني